International Journal of Control
Vol. 78, No. 12, 15 August 2005, 906–926

Subspace identification for non-linear systems with measured-input non-linearities

S. L. LACY*† and D. S. BERNSTEIN‡

†Air Force Research Laboratory, Space Vehicles Directorate, Kirtland AFB NM 87117
‡Aerospace Engineering Department, University of Michigan, Ann Arbor MI 48109

(*Received 8 September 2004; in final form 15 June 2005*)

This paper uses subspace methods to identify a class of multi-input multi-output discrete-time non-linear time-varying systems. Specifically, we identify systems that are non-linear in measured data and linear in unmeasured states. Numerical examples are presented to demonstrate the efficacy of the method.

1. Introduction

System identification is the process of constructing models based on measured data. These identified models can then be used for controller and observer design, system analysis, and output prediction. Linear system identification has been well studied (Moonen *et al*. 1989, Söderstrom and Stoica 1989, Juang 1993, Van Overschee and De Moor 1996, Larimore 1999b, Ljung 1999, Pintelon and Schoukens 2001), while non-linear system identification has received increasing attention (Larimore 1988, Chen and Fassois 1992, Greblickl 1992, 1997, Westwick and Kearney 1992, Vincent *et al*. 1994, Wigren 1994, Verhaegen and Yu 1995, Westwick and Verhaegen 1996, Al-Duwaish and Nazmul Karim 1997, Bai 1998, Johansson *et al*. 2000, Lovera *et al*. 2000, Lacy *et al*. 2001, Vöros 2001, Lacy and Bernstein 2003a, Schoukens *et al*. 2003)

Subspace identification methods have been applied to linear systems in Moonen *et al*. (1989), Verhaegen and Dewilde (1992a, b), Verhaegen (1993), Van Overschee and De Moor (1994, 1995, 1996), Deistlet *et al*. (1995), Viberg (1995), Ljung and McKelvey (1996), McKelvey *et al*. (1996), Peternell *et al*. (1996), Viberg *et al*. (1997), Johansson *et al*. (1999), Larimore (1999b), Lovera *et al*. (2001), Van Gestel *et al*. (2001), Lacy and Bernstein (2003b). Several of the most developed and widely used algorithms, CVA, N4SID, DynaMod, and MOESP, have been implemented in MATLAB packages (Haverkamp and Verhaegen 1997, Larimore 1999a, Blaurock 2003, MARLAB 2003). These methods are computationally tractable and are naturally applicable to MIMO systems. Subspace algorithms may be used to initialize more complex prediction-error and maximum likelihood methods (Larimore 1999a, Ljung 1999, Blaurock 2003, MARLAB 2003).

Several authors have extended subspace identification methods developed for identifying linear time-invariant systems to the identification of non-linear and time-varying systems. In Westwick and Verhaegen (1996) and Lovera *et al*. (2000) the authors apply subspace methods to the identification of Wiener systems. Hammerstein systems are studied in Verhaegen and Westwick (1996). Subspace identification methods are used to identify time varying systems in Verhaegen and Yu (1995). Finally, non-linear friction characteristics are investigated using subspace identification methods in Johansson *et al*. (2000).

The present paper considers non-linear systems of a particular form in which the inputs to the non-linearities are measured, or, equivalently, that are non-linear in measured data and linear in the unmeasured states, see figure 1. This specialized model structure includes classical model structures such as single-input single-output Hammerstein and non-linear feedback structures as special cases. The literature on identifying Hammerstein systems is generally confined to the single input case (Greblicki and Pawlak 1989, Al-Duwaish and Nazmul Karim 1997, Vörös 1997, Bai 1998, 2002), due in part to the need for handling arbitrary sets of basis functions. The system structure studied in this work includes

*Corresponding author. Email: seth.lacy@kirtland.af.mil

International Journal of Control
ISSN 0020–7179 print/ISSN 1366–5820 online © 2005 Taylor & Francis Group Ltd
http://www.tandf.co.uk/journals
DOI: 10.1080/00207170500214095

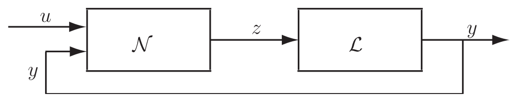

Figure 1. Non-linear system with measured-input non-linearities. $\mathcal{N}$ is a non-linear function of current and past data, and $\mathcal{L}$ is a linear dynamic system. The measured signals are u and y. The signal z is not measured.

multi-input multi-output Hammerstein systems. The number of basis functions increases with the dimension of the input vector, depending on the nature of the basis functions selected. However, the number of basis functions does not vary with the dimension of the state vector.

For non-linear systems with measured input non-linearities we rewrite the non-linear system identification problem as a linear system identification problem. The overall approach consists of three steps. First, we select a set of basis functions to approximate the non-linearities in the system. Prior knowledge of the system can be incorporated through the selection of these basis functions. We use values of the basis functions as a new set of inputs to an equivalent linear system. Next, Theorem 1 is used to estimate the state sequence in this equivalent linear system. Finally, the estimated state sequence is used to identify the unknown system parameters of the equivalent linear system using standard least squares techniques. These parameters correspond to the dynamics matrix, output matrix, and the coefficients of the non-linear basis functions of the non-linear system. Experimental application of this approach is presented in Lacy and Bernstein (2002). Methods for basis function selection and optimization are discussed in Palanth *et al.* (2004).

While many different subspace identification algorithms could be applied in the second step, we adopt the method of Moonen *et al.* (1989) and present a self-contained proof, which is not available in the literature. The proof of Theorem 1 assumes that noise is not present, which is consistent with the results given in Moonen *et al.* (1989). However, the assumptions, conclusions, and details of the proof of Theorem 1 are different from those given in Moonen *et al.* (1989). Consistency and asymptotic behaviour of several subspace methods in the presence of disturbances and measurement noise is discussed in Deistler *et al.* (1995), Peternell *et al.* (1996), Jansson and Wahlberg (1998), Bauer *et al.* (1999), Bauer and Jansson (2000), Bauer (2001), Knudsen (2001), Li and Qin (2001), Bauer and Ljung (2002), Pintelon (2002). The proof of Theorem 1 provides the basis for analyzing the effects of noise in future work.

This paper is organized as follows. The problem and the notation to be used throughout the paper is presented in § 2. The main results of the paper are derived in § 3 in the zero noise case as in Moonen *et al.* (1989). The system order and state sequence are estimated in § 4. Using the state sequence estimate, the system coefficients are calculated in § 5. Section 6 is a summary of the identification procedure. Numerical examples are presented in § 7.

2. Non-linear subspace identification

Here we study systems of the form

$$x(k+1) = Ax(k) + F(k, u(k), \ldots, u(k-b), y(k), \ldots, y(k-b)) + w(k), \quad (1)$$

$$y(k) = Cx(k) + G(k, u(k), \ldots, u(k-b), y(k-1), \ldots, y(k-b)) + Ew(k) + v(k). \quad (2)$$

The model structure (1), (2) encompasses multi-input, multi-output systems that depend linearly on the unmeasured states, but non-linearly on the time $k \in \mathbb{N}$ and the measured signals u and y. For convenience we rewrite (1), (2) as

$$x(k+1) = Ax(k) + F(k, u(k-b\colon k), y(k-b\colon k)) + w(k), \quad (3)$$

$$y(k) = Cx(k) + G(k, u(k-b\colon k), y(k-b\colon k-1)) + Ew(k) + v(k), \quad (4)$$

where we use the notation

$$a(i\colon j) \triangleq \begin{bmatrix} a(i) & \cdots & a(j) \end{bmatrix}, \quad i \le j, \quad (5)$$

b is the memory depth of $\mathcal{N}$, $u(k) \in \mathbb{R}^m$, $x(k) \in \mathbb{R}^n$, $y(k) \in \mathbb{R}^p$, $A \in \mathbb{R}^{n\times n}$, $C \in \mathbb{R}^{p\times n}$, $F\colon \mathbb{N} \times \mathbb{R}^{m\times b+1} \times \mathbb{R}^{p\times b+1} \to \mathbb{R}^n$, and $G\colon \mathbb{N} \times \mathbb{R}^{m\times b+1} \times \mathbb{R}^{p\times b} \to \mathbb{R}^p$. In addition, $w(k) \in \mathbb{R}^n$ and $v(k) \in \mathbb{R}^p$ represent state and measurement noise, respectively. The term $Ew(k)$ in (4) models correlated state and measurement noise. This model structure is illustrated by the block diagram in figure 1, where the non-linear function $\mathcal{N}$ is given by

$$\mathcal{N} \triangleq \begin{bmatrix} F \\ G \end{bmatrix}, \quad (6)$$

and the linear system $\mathcal{L}$ has the form

$$x(k+1) = Ax(k) + \begin{bmatrix} I & 0 \end{bmatrix} \mathcal{N}(k, u(k-b\colon k), y(k-b\colon k)) + w(k), \quad (7)$$

$$y(k) = Cx(k) + \begin{bmatrix} 0 & I \end{bmatrix} \mathcal{N}(k, u(k-b\colon k), y(k-b\colon k)) + Ew(k) + v(k). \quad (8)$$

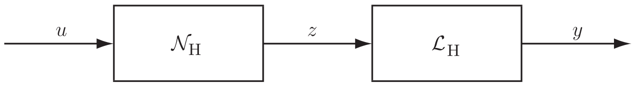

Figure 2. Hammerstein system.

The model (3), (4) includes classical model structures as special cases. For example, to capture a Hammerstein system, where the non-linearities are functions of the current input, we write (3) and (4) as

$$x(k+1) = Ax(k) + F(u(k)) + w(k), \tag{9}$$
$$y(k) = Cx(k) + G(u(k)) + Ew(k) + v(k), \tag{10}$$

illustrated in figure 2, where the non-linear function $\mathcal{N}_\mathrm{H}$ is given by

$$\mathcal{N}_\mathrm{H} \triangleq \begin{bmatrix} F \\ G \end{bmatrix}, \tag{11}$$

and the linear system $\mathcal{L}_\mathrm{H}$ has the form

$$x(k+1) = Ax(k) + \begin{bmatrix} I & 0 \end{bmatrix}\mathcal{N}_\mathrm{H}(u(k)) + w(k), \tag{12}$$
$$y(k) = Cx(k) + \begin{bmatrix} 0 & I \end{bmatrix}\mathcal{N}_\mathrm{H}(u(k)) + Ew(k) + v(k). \tag{13}$$

Note that the literature for identifying Hammerstein systems is generally confined to the single input case (Greblicki and Pawlak 1989, Al-Duwaish and Nazmul Karim 1997, Vörös 1997, Bai 1998, 2002), while the system structure presented in this work encompasses multi-input multi-output Hammerstein systems due to the multi-input multi-output nature of subspace identification algorithms. For a non-linear feedback system, we write (3), (4) as

$$x(k+1) = Ax(k) + Bu(k) + F(y(k)) + w(k), \tag{14}$$
$$y(k) = Cx(k) + Du(k) + Ew(k) + v(k), \tag{15}$$

illustrated in figure 3, where

$$\mathcal{N}_\mathrm{NLF} \triangleq F, \tag{16}$$

and $\mathcal{L}_\mathrm{NLF}$ represents the linear system

$$x(k+1) = Ax(k) + Bu(k) + \mathcal{N}_\mathrm{NLF}(y(k)) + w(k), \tag{17}$$
$$y(k) = Cx(k) + Du(k) + Ew(k) + v(k). \tag{18}$$

We assume that F and G can be represented as linear combinations of a finite set of known basis functions $f_i\colon \mathbb{N} \times \mathbb{R}^{m\times b+1} \times \mathbb{R}^{p\times b+1} \to \mathbb{R}$, $i = 1, \ldots, r$, $g_i\colon \mathbb{N} \times \mathbb{R}^{m\times b+1} \times \mathbb{R}^{p\times b} \to \mathbb{R}$, $i = 1, \ldots, s$, and $h_i\colon \mathbb{N} \times \mathbb{R}^{m\times b+1} \times \mathbb{R}^{p\times b} \to \mathbb{R}$, $i = 1, \ldots, t$, with unknown matrix

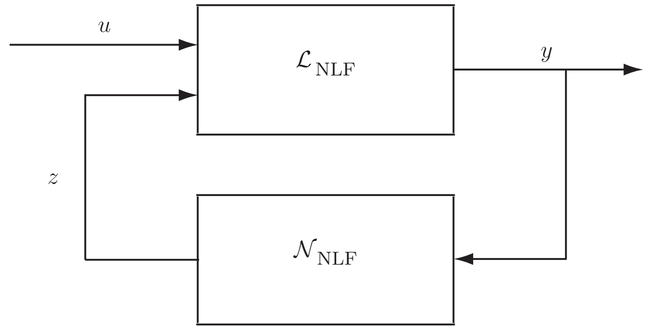

Figure 3. A non-linear feedback system.

coefficients $B_1 \in \mathbb{R}^{n\times r}$, $D_1 \in \mathbb{R}^{p\times s}$, $B_2 \in \mathbb{R}^{n\times t}$, and $D_2 \in \mathbb{R}^{p\times t}$ such that

$$\begin{aligned} &F(k, u(k-b\colon k), y(k-b\colon k)) \\ &\quad = B_1 f(k, u(k-b\colon k), y(k-b\colon k)) \\ &\qquad + B_2 h(k, u(k-b\colon k), y(k-b\colon k-1)), \end{aligned} \tag{19}$$

$$\begin{aligned} &G(k, u(k-b\colon k), y(k-b\colon k-1)) \\ &\quad = D_1 g(k, u(k-b\colon k), y(k-b\colon k-1)) \\ &\qquad + D_2 h(k, u(k-b\colon k), y(k-b\colon k-1)), \end{aligned} \tag{20}$$

where

$$f(k, u(k-b\colon k), y(k-b\colon k)) \triangleq \begin{bmatrix} f_1(k, u(k-b\colon k), y(k-b\colon k)) \\ \vdots \\ f_r(k, u(k-b\colon k), y(k-b\colon k)) \end{bmatrix}, \tag{21}$$

$$g(k, u(k-b\colon k), y(k-b\colon k-1)) \triangleq \begin{bmatrix} g_1(k, u(k-b\colon k), y(k-b\colon k-1)) \\ \vdots \\ g_s(k, u(k-b\colon k), y(k-b\colon k-1)) \end{bmatrix}, \tag{22}$$

$$h(k, u(k-b\colon k), y(k-b\colon k-1)) \triangleq \begin{bmatrix} h_1(k, u(k-b\colon k), y(k-b\colon k-1)) \\ \vdots \\ h_t(k, u(k-b\colon k), y(k-b\colon k-1)) \end{bmatrix}, \tag{23}$$

and r, s, and t are the number of basis functions in each expansion. Note that g and h are functions of past outputs only, while f is a function of both past outputs and the current output. If the functions F and G cannot be exactly represented as a finite sum of basis functions, the expansions (19) and (20) can be regarded as approximations. The same set of basis functions can be used for any choice of state dimension. The number $\sigma \triangleq r+s+t$ of basis functions required does not increase with n. The basis functions in f, g, and h are sorted according to whether they appear in the expansion of F, G, or both. Specifically, f is a list of the basis functions that appear only in the expansion of F; g is a list of the basis functions that appear only in the expansion of G; and h is a list of the basis functions that appear in the expansions of both F and G. Without this convention, $\tilde{Z}_q(k)$ defined below could not have full row rank. Methods for selecting and refining the set of basis functions f_i, g_i and h_i are discussed in Palanth *et al.* (2004).

With the notation (19), (20) we can rewrite (3) and (4) as

$$\begin{aligned} x(k+1) = {} & Ax(k) + B_1 f(k, u(k-b{:}\,k), y(k-b{:}\,k)) \\ & + B_2 h(k, u(k-b{:}\,k), y(k-b{:}\,k-1)) + w(k), \end{aligned} \tag{24}$$

$$\begin{aligned} y(k) = {} & Cx(k) + D_1 g(k, u(k-b{:}\,k), y(k-b{:}\,k-1)) \\ & + D_2 h(k, u(k-b{:}\,k), y(k-b{:}\,k-1)) \\ & + Ew(k) + v(k), \end{aligned} \tag{25}$$

illustrated in figure 4, where

$$\tilde{\mathcal{N}} \triangleq \begin{bmatrix} f \\ g \\ h \end{bmatrix}, \tag{26}$$

and $\tilde{\mathcal{L}}$ represents the system

$$\begin{aligned} x(k+1) = {} & Ax(k) + \begin{bmatrix} B_1 & 0 & B_2 \end{bmatrix} \\ & \times \tilde{\mathcal{N}}(k, u(k-b{:}\,k), y(k-b{:}\,k)), \end{aligned} \tag{27}$$

$$\begin{aligned} y(k) = {} & Cx(k) + \begin{bmatrix} 0 & D_1 & D_2 \end{bmatrix} \\ & \times \tilde{\mathcal{N}}(k, u(k-b{:}\,k), y(k-b{:}\,k)). \end{aligned} \tag{28}$$

Using (24) and (25), we construct the block-matrix equation

$$Y_q(k) = \Gamma_q x(k{:}\,k+\ell-2q) + \Lambda_q \tilde{Z}_q(k) + \Upsilon_q N_q(k), \tag{29}$$

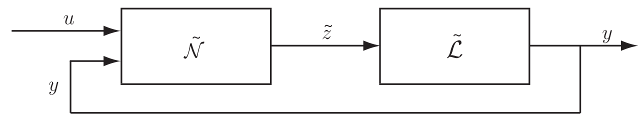

Figure 4. Equivalent block diagram of a system linear in unmeasured states. In this formulation, $\tilde{\mathcal{N}}$ is a non-linear function of current and past data, and $\tilde{\mathcal{L}}$ is a linear dynamic system.

where q is a user-defined window length denoting the number of block rows in (29). The number of columns in (29) is $\ell-2q+1$, where ℓ is a second user-defined window length. In practice, ℓ may be taken to be the number of measurements of u and y available for use in the identification. In (29), we define the block-Hankel matrix $Y_q(k) \in \mathbb{R}^{pq \times \ell-2q+1}$ as

$$Y_q(k) \triangleq \begin{bmatrix} y(k{:}\,k+\ell-2q) \\ y(k+1{:}\,k+\ell-2q+1) \\ \vdots \\ y(k+q-1{:}\,k+\ell-q-1) \end{bmatrix},$$

the extended observability matrix $\Gamma_q \in \mathbb{R}^{pq \times n}$ as

$$\Gamma_q \triangleq \begin{bmatrix} C \\ CA \\ CA^2 \\ \vdots \\ CA^{q-1} \end{bmatrix},$$

the block-Toeplitz matrix $\Lambda_q \in \mathbb{R}^{pq \times q\sigma}$ as

$$\Lambda_q \triangleq \begin{bmatrix} 0 & D_1 & D_2 & 0 & 0 & 0 & \cdots & 0 \\ CB_1 & 0 & CB_2 & 0 & D_1 & D_2 & \cdots & 0 \\ CAB_1 & 0 & CAB_2 & CB_1 & 0 & CB_2 & \cdots & 0 \\ CA^2B_1 & 0 & CA^2B_2 & CAB_1 & 0 & CAB_2 & \cdots & 0 \\ \vdots & \vdots & \vdots & \vdots & \vdots & \vdots & & \vdots \\ CA^{q-2}B_1 & 0 & CA^{q-2}B_2 & CA^{q-3}B_1 & 0 & CA^{q-3}B_2 & \cdots & D_2 \end{bmatrix},$$

the block-Hankel matrix $\tilde{Z}_q(k) \in \mathbb{R}^{q\sigma \times \ell-2q+1}$ as

$$\tilde{Z}_q(k) \triangleq \begin{bmatrix} \tilde{z}(k{:}\,k+\ell-2q) \\ \tilde{z}(k+1{:}\,k+\ell-2q+1) \\ \vdots \\ \tilde{z}(k+q-1{:}\,k+\ell-q-1) \end{bmatrix},$$

the column vector $\tilde{z}(k) \in \mathbb{R}^{\sigma}$ as

$$\tilde{z}(k) \triangleq \begin{bmatrix} f(k, u(k-b:k), y(k-b:k)) \\ g(k, u(k-b:k), y(k-b:k-1)) \\ h(k, u(k-b:k), y(k-b:k-1)) \end{bmatrix},$$

the block-Toeplitz matrix $\Upsilon_q \in \mathbb{R}^{pq \times q(n+p)}$ as

$$\Upsilon_q \triangleq \begin{bmatrix} E & I & 0 & 0 & 0 & 0 & \cdots & 0 \\ C & 0 & E & I & 0 & 0 & \cdots & 0 \\ CA & 0 & C & 0 & E & I & \cdots & 0 \\ CA^2 & 0 & CA & 0 & C & 0 & \cdots & 0 \\ \vdots & \vdots & \vdots & \vdots & \vdots & \vdots & & \vdots \\ CA^{q-2} & 0 & CA^{q-3} & 0 & CA^{q-4} & 0 & \cdots & I \end{bmatrix},$$

and the block-Hankel matrix $N_q(k) \in \mathbb{R}^{q(n+p) \times \ell-2q+1}$ as

$$N_q(k) \triangleq \begin{bmatrix} w(k:k+\ell-2q) \\ v(k:k+\ell-2q) \\ w(k+1:k+\ell-2q+1) \\ v(k+1:k+\ell-2q+1) \\ \vdots \\ w(k+q-1:k+\ell-q-1) \\ v(k+q-1:k+\ell-q-1) \end{bmatrix}.$$

Finally, we define the data matrix $\Delta_q(k) \in \mathbb{R}^{q(p+\sigma) \times \ell-2q+1}$ as

$$\Delta_q(k) \triangleq \begin{bmatrix} Y_q(k) \\ \tilde{Z}_q(k) \end{bmatrix}. \tag{30}$$

3. State reconstruction

In this section, we give conditions under which the state sequence $x(k+q:k+\ell-q)$ can be reconstructed to within an unknown coordinate transformation using measured data. For $V \in \mathbb{R}^{n \times m}$ let $\mathcal{R}(V)$ denote the range (column space) of V. Then $\mathcal{R}(V^{\mathrm{T}})$ is the row space of V. Let $V^{\mathrm{L}} \triangleq (V^{\mathrm{T}}V)^{-1}V^{\mathrm{T}}$ and $V^{\mathrm{R}} \triangleq V^{\mathrm{T}}(VV^{\mathrm{T}})^{-1}$ denote left and right inverses of V, respectively. We also define $\Pi_V \triangleq V^{\mathrm{R}}V = V^{\mathrm{T}}(VV^{\mathrm{T}})^{-1}V$ and $\Pi_V^{\perp} \triangleq I - \Pi_V$ such that $V\Pi_V = V$ and $V\Pi_V^{\perp} = 0$.

Theorem 1: *Assume the following conditions are satisfied:*

(i) $\operatorname{rank} \Gamma_q = n$.
(ii) *$w(k)$ and $v(k)$ are zero for all $k \in \mathbb{N}$.*
(iii) $\operatorname{rank}\left[\tilde{Z}_q(k)\ \ \tilde{Z}_q(k+q)\right] = 2q\sigma$ *for all* $k \in \mathbb{N}$.
(iv) $\operatorname{rank}(x(k:k+\ell-2q)\Pi^{\perp}_{\tilde{Z}_q(k)}) = \operatorname{rank} x(k:k+\ell-2q)$ *for all* $k \in \mathbb{N}$.
(v) $\operatorname{rank} x(k:k+\ell-4q) = n$ *for all* $k \in \mathbb{N}$.
(vi) $\operatorname{rank}(x(k:k+\ell-4q)\Pi^{\perp}_{\tilde{Z}_{2q}(k)}) = \operatorname{rank} x(k:k+\ell-4q)$ *for all* $k \in \mathbb{N}$.

Then

$$q \geq n/p, \tag{31}$$

$$\ell \geq 2q(\sigma+1)+n-1, \tag{32}$$

$$\operatorname{rank}\begin{bmatrix} \Delta_q(k) \\ \Delta_q(k+q) \end{bmatrix} = 2q\sigma + n \quad \text{for all } k \in \mathbb{N}, \tag{33}$$

and

$$\mathcal{R}(x^{\mathrm{T}}(k+q:k+\ell-q)) = \mathcal{R}\left(\Delta_q^{\mathrm{T}}(k)\right) \bigcap \mathcal{R}\left(\Delta_q^{\mathrm{T}}(k+q)\right) \quad \text{for all } k \in \mathbb{N}. \tag{34}$$

Proof: (31) follows directly from (i). We shall prove (32) and (33) in the course of proving (30). To prove (34) we first show that (35) holds with "=" replaced with "⊆". Then the left and right hand sides of (34) will be shown to have the same dimension. Let $k \in \mathbb{N}$.

First, (ii) implies that (29) has the form

$$Y_q(k) = \Gamma_q x(k:k+\ell-2q) + \Lambda_q \tilde{Z}_q(k) \tag{35}$$

and

$$Y_q(k+q) = \Gamma_q x(k+q:k+\ell-q) + \Lambda_q \tilde{Z}_q(k+q). \tag{36}$$

By (i) we can solve (35) and (36) for the state matrices

$$x(k:k+\ell-2q) = \begin{bmatrix} \Gamma_q^{\mathrm{L}} & -\Gamma_q^{\mathrm{L}}\Lambda_q \end{bmatrix} \Delta_q(k) \tag{37}$$

and

$$x(k+q:k+\ell-q) = \begin{bmatrix} \Gamma_q^{\mathrm{L}} & -\Gamma_q^{\mathrm{L}}\Lambda_q \end{bmatrix} \Delta_q(k+q). \tag{38}$$

Using (24), (37) and (ii), the state matrix $x(k+q:k+\ell-q)$ can also be written as

$$\begin{aligned} x(k+q:k+\ell-q) &= A^q x(k:k+\ell-2q) + \Psi_q \tilde{Z}_q(k) \\ &= A^q \begin{bmatrix} \Gamma_q^{\mathrm{L}} & -\Gamma_q^{\mathrm{L}}\Lambda_q \end{bmatrix} \Delta_q(k) + \Psi_q \tilde{Z}_q(k) \\ &= \begin{bmatrix} A^q\Gamma_q^{\mathrm{L}} & \Psi_q - A^q\Gamma_q^{\mathrm{L}}\Lambda_q \end{bmatrix} \Delta_q(k), \end{aligned} \tag{39}$$

where $\Psi_q \in \mathbb{R}^{n\times q\sigma}$ is defined as

$$\Psi_q \triangleq \left[A^{q-1}\left[B_1\ \ 0\ \ B_2\right]\ A^{q-2}\left[B_1\ \ 0\ \ B_2\right]\ \cdots\ \left[B_1\ \ 0\ \ B_2\right]\right]. \tag{40}$$

Now (38) and (39) imply

$$\mathcal{R}\big(x^{\mathrm{T}}(k+q\colon k+\ell-q)\big) \subseteq \mathcal{R}\Big(\Delta_q^{\mathrm{T}}(k)\Big)\bigcap\mathcal{R}\Big(\Delta_q^{\mathrm{T}}(k+q)\Big). \tag{41}$$

Hence (34) holds with "=" replaced with "⊆".

Next we show that the left and right hand sides of (34) have the same dimension. By (iii), it follows that $\operatorname{rank}\tilde{Z}_q(k) = q\sigma$ and thus $\Pi^{\perp}_{\tilde{Z}_q(k)}$ exists. Multiplying (35) on the right by $\Pi^{\perp}_{\tilde{Z}_q(k)}$ and using $\tilde{Z}_q(k)\Pi^{\perp}_{\tilde{Z}_q(k)} = 0$ yields

$$Y_q(k)\Pi^{\perp}_{\tilde{Z}_q(k)} = \Gamma_q x(k\colon k+\ell-2q)\Pi^{\perp}_{\tilde{Z}_q(k)}. \tag{42}$$

Using (42), (i), (iv), and (v) it follows that

$$\begin{aligned}\operatorname{rank}\Big(Y_q(k)\Pi^{\perp}_{\tilde{Z}_q(k)}\Big) &= \operatorname{rank}\Big(\Gamma_q x(k\colon k+\ell-2q)\Pi^{\perp}_{\tilde{Z}_q(k)}\Big)\\ &= \operatorname{rank}\Big(x(k\colon k+\ell-2q)\Pi^{\perp}_{\tilde{Z}_q(k)}\Big)\\ &= \operatorname{rank} x(k\colon k+\ell-2q)\\ &= n.\end{aligned} \tag{43}$$

Using (43), $\mathcal{R}(\Pi_{\tilde{Z}_q(k)}Y_q^{\mathrm{T}}(k)) \subseteq \mathcal{R}(\Pi_{\tilde{Z}_q(k)}) = \mathcal{R}(\tilde{Z}_q^{\mathrm{T}}(k))$, $\tilde{Z}_q(k)\Pi^{\perp}_{\tilde{Z}_q(k)}Y_q^{\mathrm{T}}(k) = 0$, and (iii) we can now calculate

$$\begin{aligned}\operatorname{rank}(\Delta_q(k)) &= \operatorname{rank}\begin{bmatrix}Y_q(k)\\ \tilde{Z}_q(k)\end{bmatrix}\\ &= \operatorname{rank}\begin{bmatrix}Y_q(k)\Big(\Pi_{\tilde{Z}_q(k)}+\Pi^{\perp}_{\tilde{Z}_q(k)}\Big)\\ \tilde{Z}_q(k)\end{bmatrix}\\ &= \operatorname{rank}\Big[\Pi_{\tilde{Z}_q(k)}Y_q^{\mathrm{T}}(k)+\Pi^{\perp}_{\tilde{Z}_q(k)}Y_q^{\mathrm{T}}(k)\quad \tilde{Z}_q^{\mathrm{T}}(k)\Big]\\ &= \operatorname{rank}\Big[\Pi^{\perp}_{\tilde{Z}_q(k)}Y_q^{\mathrm{T}}(k)\quad \tilde{Z}_q^{\mathrm{T}}(k)\Big]\\ &= \operatorname{rank}(\tilde{Z}_q(k)) + \operatorname{rank}\Big(Y_q(k)\Pi^{\perp}_{\tilde{Z}_q(k)}\Big)\\ &= q\sigma + n.\end{aligned} \tag{44}$$

Replacing k by $k+q$ in (44) yields

$$\operatorname{rank}\big(\Delta_q(k+q)\big) = q\sigma + n. \tag{45}$$

As in (43) and (44) and using (vi) we calculate

$$\begin{aligned}\operatorname{rank}\Big(Y_{2q}(k)\Pi^{\perp}_{\tilde{Z}_{2q}(k)}\Big) &= \operatorname{rank}\Big(\Gamma_{2q}x(k\colon k+\ell-4q)\Pi^{\perp}_{\tilde{Z}_{2q}(k)}\Big)\\ &= \operatorname{rank}\Big(x(k\colon k+\ell-4q)\Pi^{\perp}_{\tilde{Z}_{2q}(k)}\Big)\\ &= \operatorname{rank} x(k\colon k+\ell-4q)\\ &= n,\end{aligned} \tag{46}$$

to find

$$\begin{aligned}&\operatorname{rank}(\Delta_{2q}(k))\\ &\quad= \operatorname{rank}\begin{bmatrix}Y_{2q}(k)\\ \tilde{Z}_{2q}(k)\end{bmatrix}\\ &\quad= \operatorname{rank}\begin{bmatrix}Y_{2q}(k)\Big(\Pi_{\tilde{Z}_{2q}(k)}+\Pi^{\perp}_{\tilde{Z}_{2q}(k)}\Big)\\ \tilde{Z}_{2q}(k)\end{bmatrix}\\ &\quad= \operatorname{rank}\Big[\Pi_{\tilde{Z}_{2q}(k)}Y_{2q}^{\mathrm{T}}(k)+\Pi^{\perp}_{\tilde{Z}_{2q}(k)}Y_{2q}^{\mathrm{T}}(k)\quad \tilde{Z}_{2q}^{\mathrm{T}}(k)\Big]\\ &\quad= \operatorname{rank}\Big[\Pi^{\perp}_{\tilde{Z}_{2q}(k)}Y_{2q}^{\mathrm{T}}(k)\quad \tilde{Z}_{2q}^{\mathrm{T}}(k)\Big]\\ &\quad= \operatorname{rank}(\tilde{Z}_{2q}(k)) + \operatorname{rank}\Big(Y_{2q}(k)\Pi^{\perp}_{\tilde{Z}_{2q}(k)}\Big)\\ &\quad= 2q\sigma + n.\end{aligned} \tag{47}$$

Noting

$$\tilde{Z}_{2q}(k) = \begin{bmatrix}\tilde{Z}_q(k)\\ \tilde{Z}_q(k+q)\end{bmatrix} \quad\text{and}\quad Y_{2q}(k) = \begin{bmatrix}Y_q(k)\\ Y_q(k+q)\end{bmatrix}$$

and using (47) we obtain

$$\begin{aligned}\operatorname{rank}\begin{bmatrix}\Delta_q(k)\\ \Delta_q(k+q)\end{bmatrix} &= \operatorname{rank}\begin{bmatrix}Y_q(k)\\ \tilde{Z}_q(k)\\ Y_q(k+q)\\ \tilde{Z}_q(k+q)\end{bmatrix}\\ &= \operatorname{rank}\begin{bmatrix}Y_q(k)\\ Y_q(k+q)\\ \tilde{Z}_q(k)\\ \tilde{Z}_q(k+q)\end{bmatrix}\\ &= \operatorname{rank}\begin{bmatrix}Y_{2q}(k)\\ \tilde{Z}_{2q}(k)\end{bmatrix}\\ &= \operatorname{rank}(\Delta_{2q}(k))\\ &= 2q\sigma + n.\end{aligned} \tag{48}$$

This proves (33). Also, since

$$\begin{bmatrix} \Delta_q(k) \\ \Delta_q(k+q) \end{bmatrix} \in \mathbb{R}^{2q(p+\sigma)\times \ell-2q+1}$$

it follows that $2q\sigma + n \le \ell - 2q + 1$, which proves (32).

Finally, using (44), (45), (48), and (v) we compute the dimension of the right hand side of (47) to be

$$\begin{aligned} \dim\Big(\mathcal{R}\Big(\Delta_q^{\mathrm{T}}(k)\Big) \bigcap \mathcal{R}\Big(\Delta_q^{\mathrm{T}}(k+q)\Big)\Big) &= \operatorname{rank}(\Delta_q(k)) + \operatorname{rank}(\Delta_q(k+q)) \\ &\quad - \operatorname{rank}\begin{bmatrix} \Delta_q(k) \\ \Delta_q(k+q) \end{bmatrix} \\ &= q\sigma + n + q\sigma + n - (2q\sigma + n) \\ &= n \\ &= \operatorname{rank} x(k+q\colon k+\ell-q) \\ &= \dim \mathcal{R}(x^{\mathrm{T}}(k+q\colon k+\ell-q)), \end{aligned} \tag{49}$$

which proves (34).

In the next result, we propose a direct computation of the intersection of the row spaces of $\Delta_q(k)$ and $\Delta_q(k+q)$.

Proposition 1: *Let $k \in \mathbb{N}$ and assume that* (i)–(vi) *of Theorem* 1 *are satisfied. Then*

$$\mathcal{R}(\delta^{\mathrm{T}}(k)) = \mathcal{R}\Big(\Delta_q^{\mathrm{T}}(k)\Big) \bigcap \mathcal{R}\Big(\Delta_q^{\mathrm{T}}(k+q)\Big), \tag{50}$$

where $\delta(k) \in \mathbb{R}^{\ell-2q+1\times \ell-2q+1}$ given by

$$\begin{aligned} \delta(k) &\triangleq 2\Delta_q^{+}(k)\Delta_q(k)(\Delta_q^{+}(k)\Delta_q(k) + \Delta_q^{+}(k+q)\Delta_q(k+q))^{+} \\ &\quad \times \Delta_q^{+}(k+q)\Delta_q(k+q), \end{aligned} \tag{51}$$

see Anderson Jr and Duffin (1969). *Then there exists non-singular $T \in \mathbb{R}^{n\times n}$ such that*

$$x(k+q\colon k+\ell-q) = TU_\delta^{\mathrm{T}}(k)\delta(k), \tag{52}$$

where $U_\delta(k) \in \mathbb{R}^{\ell-2q+1\times n}$ is defined through the singular value decomposition

$$\delta(k) = \begin{bmatrix} U_\delta(k) & U_\eta(k) \end{bmatrix} \begin{bmatrix} S_\delta(k) & 0 \\ 0 & 0 \end{bmatrix} V_\delta^{\mathrm{T}}(k), \tag{53}$$

and $U_\eta(k) \in \mathbb{R}^{\ell-2q+1\times \ell-2q-n+1}$, $S_\delta(k) \in \mathbb{R}^{n\times n}$, and $V_\delta(k) \in \mathbb{R}^{\ell-2q+1\times \ell-2q+1}$.

The calculation of the state sequence (52), while direct, requires forming the large matrix $\delta(k) \in \mathbb{R}^{\ell-2q+1\times \ell-2q+1}$. In addition, in the presence of noise, the row spaces of $\Delta_q(k)$ and $\Delta_q(k+q)$ will generally intersect only at the origin, in which case δ(k) will have rank near zero! Therefore, when noise is present, we would like an approximation to this intersection. Under additional conditions, Propositions 2 and 3 below provide useful approximations to the intersections of the row spaces of $\Delta_q(k)$ and $\Delta_q(k+q)$.

The result (34) implies that, for all $k \in \mathbb{N}$, there exist matrices $M_1 \in \mathbb{R}^{n\times q(p+\sigma)}$ and $M_2 \in \mathbb{R}^{n\times q(p+\sigma)}$ such that

$$x(k+q\colon k+\ell-q) = M_1\Delta_q(k) = M_2\Delta_q(k+q). \tag{54}$$

If either M_1 or M_2 were known, (54) could be used to obtain the state sequence directly from measured data. The goal of Proposition 2 is to estimate M_1 and M_2.

In the following result we suppress the dependence of the matrices T, U_{11}, U_{12}, U_{21}, U_{22}, S_{11}, V, U_r, U_s, S_r, V_r, and V_s on the time step k for notational convenience and clarity. If k is taken to be 1, then the last data used in the algorithm occurs at $k = \ell$.

Proposition 2: *Let $k \in \mathbb{N}$ and assume that* (i)–(vi) *of Theorem* 1 *are satisfied. Let $M \in \mathbb{R}^{\ell-2q+1\times c_M}$ be non-singular, and let*

$$L = \begin{bmatrix} L_{11} & L_{12} \\ L_{21} & L_{22} \end{bmatrix} \in \mathbb{R}^{2q(p+\sigma)\times 2q(p+\sigma)},$$

where L_{11}, L_{12}, L_{21}, and $L_{22} \in \mathbb{R}^{q(p+\sigma)\times q(p+\sigma)}$, and L_{11}, L_{22}, $L_{11} - L_{12}L_{22}^{-1}L_{21}$, and $L_{22} - L_{21}L_{11}^{-1}L_{12}$ are non-singular. Consider the singular value decomposition

$$L\begin{bmatrix} \Delta_q(k) \\ \Delta_q(k+q) \end{bmatrix} M = \begin{bmatrix} U_{11} & U_{12} \\ U_{21} & U_{22} \end{bmatrix} \begin{bmatrix} S_{11} & 0 \\ 0 & 0 \end{bmatrix} V^{\mathrm{T}}, \tag{55}$$

where $S_{11} \in \mathbb{R}^{2q\sigma+n\times 2q\sigma+n}$, $U_{11} \in \mathbb{R}^{q(p+\sigma)\times 2q\sigma+n}$, $U_{12} \in \mathbb{R}^{q(p+\sigma)\times 2pq-n}$, $U_{21} \in \mathbb{R}^{q(p+\sigma)\times 2q\sigma+n}$, $U_{22} \in \mathbb{R}^{q(p+\sigma)\times 2pq-n}$, and $V \in \mathbb{R}^{\ell-2q+1\times \ell-2q+1}$. Let $U_l \in \mathbb{R}^{2pq-n\times n}$, $S_l \in \mathbb{R}^{n\times n}$, and $V_l \in \mathbb{R}^{2q\sigma+n\times n}$ be defined through the singular value decomposition

$$\begin{aligned} &\big(U_{12}^{\mathrm{T}}L_{11} + U_{22}^{\mathrm{T}}L_{21}\big)\Big[\big(L_{11} - L_{12}L_{22}^{-1}L_{21}\big)^{-1}U_{11} \\ &\qquad - L_{11}^{-1}L_{21}\big(L_{22} - L_{21}L_{11}^{-1}L_{12}\big)^{-1}U_{21}\Big]S_{11} \\ &= \begin{bmatrix} U_l & U_e \end{bmatrix} \begin{bmatrix} S_l & 0 \\ 0 & 0 \end{bmatrix} \begin{bmatrix} V_l^{\mathrm{T}} \\ V_e^{\mathrm{T}} \end{bmatrix} = U_lS_lV_l^{\mathrm{T}}. \end{aligned} \tag{56}$$

Furthermore, let $U_r \in \mathbb{R}^{2pq-n\times n}$, $S_r \in \mathbb{R}^{n\times n}$, *and* $V_r \in \mathbb{R}^{2q\sigma+n\times n}$ *be defined through the singular value decomposition*

$$\begin{aligned}\left(U_{12}^{\mathrm{T}}L_{12}+U_{22}^{\mathrm{T}}L_{22}\right)\Big[L_{22}^{-1}L_{21}\left(L_{11}-L_{12}L_{22}^{-1}L_{21}\right)^{-1}U_{11}\\ -\left(L_{22}-L_{21}L_{11}^{-1}L_{12}\right)^{-1}U_{21}\Big]S_{11}\\ =\begin{bmatrix}U_r & U_i\end{bmatrix}\begin{bmatrix}S_r & 0\\ 0 & 0\end{bmatrix}\begin{bmatrix}V_r^{\mathrm{T}}\\ V_i^{\mathrm{T}}\end{bmatrix}=U_rS_rV_r^{\mathrm{T}}.\end{aligned}\tag{57}$$

Finally, assume that

$$\begin{aligned}&\operatorname{rank}\left(U_{12}^{\mathrm{T}}L_{11}+U_{22}^{\mathrm{T}}L_{21}\right)\Delta_q(k)\\ &\quad=\operatorname{rank}\left(U_{12}^{\mathrm{T}}L_{12}+U_{22}^{\mathrm{T}}L_{22}\right)\Delta_q(k+q)=n.\end{aligned}\tag{58}$$

Then there exists non-singular $T \in \mathbb{R}^{n\times n}$ *such that*

$$\begin{aligned}&x(k+q\colon k+\ell-q)\\ &\quad=TU_l^{\mathrm{T}}\left(U_{12}^{\mathrm{T}}L_{11}+U_{22}^{\mathrm{T}}L_{21}\right)\Delta_q(k)\\ &\quad=T\begin{bmatrix}S_rV_r^{\mathrm{T}} & 0\end{bmatrix}V^{\mathrm{T}}M^{-1}\\ &\quad=T\begin{bmatrix}S_lV_l^{\mathrm{T}} & 0\end{bmatrix}V^{\mathrm{T}}M^{-1}\\ &\quad=-TU_r^{\mathrm{T}}\left(U_{12}^{\mathrm{T}}L_{12}+U_{22}^{\mathrm{T}}L_{22}\right)\Delta_q(k+q).\end{aligned}\tag{59}$$

Proof: First we rewrite the singular value decomposition (55) as

$$\begin{bmatrix}U_{11}^{\mathrm{T}} & U_{21}^{\mathrm{T}}\\ U_{12}^{\mathrm{T}} & U_{22}^{\mathrm{T}}\end{bmatrix}\begin{bmatrix}L_{11} & L_{12}\\ L_{21} & L_{22}\end{bmatrix}\begin{bmatrix}\Delta_q(k)\\ \Delta_q(k+q)\end{bmatrix}=\begin{bmatrix}S_{11} & 0\\ 0 & 0\end{bmatrix}V^{\mathrm{T}}M^{-1},\tag{60}$$

$$\begin{aligned}\begin{bmatrix}\Delta_q(k)\\ \Delta_q(k+q)\end{bmatrix}&=L^{-1}\begin{bmatrix}U_{11} & U_{12}\\ U_{21} & U_{22}\end{bmatrix}\begin{bmatrix}S_{11} & 0\\ 0 & 0\end{bmatrix}V^{\mathrm{T}}M^{-1}=\begin{bmatrix}\left(L_{11}-L_{12}L_{22}^{-1}L_{21}\right)^{-1} & -L_{11}^{-1}L_{12}\left(L_{22}-L_{21}L_{11}^{-1}L_{12}\right)^{-1}\\ -L_{22}^{-1}L_{21}\left(L_{11}-L_{12}L_{22}^{-1}L_{21}\right)^{-1} & \left(L_{22}-L_{21}L_{11}^{-1}L_{12}\right)^{-1}\end{bmatrix}\\ &\times\begin{bmatrix}U_{11}S_{11} & 0\\ U_{21}S_{11} & 0\end{bmatrix}V^{\mathrm{T}}M^{-1}=\begin{bmatrix}\left(L_{11}-L_{12}L_{22}^{-1}L_{21}\right)^{-1}U_{11}S_{11}-L_{11}^{-1}L_{21}\left(L_{22}-L_{21}L_{11}^{-1}L_{12}\right)^{-1}U_{21}S_{11} & 0\\ -L_{22}^{-1}L_{21}\left(L_{11}-L_{12}L_{22}^{-1}L_{21}\right)^{-1}U_{11}S_{11}+\left(L_{22}-L_{21}L_{11}^{-1}L_{12}\right)^{-1}U_{21}S_{11} & 0\end{bmatrix}V^{\mathrm{T}}M^{-1}.\end{aligned}\tag{66}$$

so that

$$\begin{bmatrix}U_{11}^{\mathrm{T}}\left[L_{11}\Delta_q(k)+L_{12}\Delta_q(k+q)\right]\\ \quad+U_{21}^{\mathrm{T}}\left[L_{21}\Delta_q(k)+L_{22}\Delta_q(k+q)\right]\\ U_{12}^{\mathrm{T}}\left[L_{11}\Delta_q(k)+L_{12}\Delta_q(k+q)\right]\\ \quad+U_{22}^{\mathrm{T}}\left[L_{21}\Delta_q(k)+L_{22}\Delta_q(k+q)\right]\end{bmatrix}=\begin{bmatrix}S_{11} & 0\\ 0 & 0\end{bmatrix}V^{\mathrm{T}}M^{-1}.\tag{61}$$

We thus have

$$\begin{aligned}&\left(U_{12}^{\mathrm{T}}L_{11}+U_{22}^{\mathrm{T}}L_{21}\right)\Delta_q(k)\\ &\quad=-\left(U_{12}^{\mathrm{T}}L_{12}+U_{22}^{\mathrm{T}}L_{22}\right)\Delta_q(k+q).\end{aligned}\tag{62}$$

Hence, (62) and (34) imply that

$$\begin{aligned}&\mathcal{R}\Big(\left(\left(U_{12}^{\mathrm{T}}L_{11}+U_{22}^{\mathrm{T}}L_{21}\right)\Delta_q(k)\right)^{\mathrm{T}}\Big)\\ &\quad\subset\mathcal{R}\Big(\Delta_q^{\mathrm{T}}(k)\Big)\bigcap\mathcal{R}\Big(\Delta_q^{\mathrm{T}}(k+q)\Big)\\ &\quad=\mathcal{R}\left(x^{\mathrm{T}}(k+q\colon k-q+\ell)\right)\end{aligned}\tag{63}$$

and

$$\begin{aligned}&\mathcal{R}\Big(\left(\left(U_{12}^{\mathrm{T}}L_{12}+U_{22}^{\mathrm{T}}L_{22}\right)\Delta_q(k+q)\right)^{\mathrm{T}}\Big)\\ &\quad\subset\mathcal{R}\Big(\Delta_q^{\mathrm{T}}(k)\Big)\bigcap\mathcal{R}\Big(\Delta_q^{\mathrm{T}}(k+q)\Big)\\ &\quad=\mathcal{R}\left(x^{\mathrm{T}}(k+q\colon k-q+\ell)\right).\end{aligned}\tag{64}$$

Furthermore, (v) and (58) imply that the left and right hand sides of (63) and (64) have the same dimension n. Therefore,

$$\begin{aligned}&\mathcal{R}\Big(\left(\left(U_{12}^{\mathrm{T}}L_{11}+U_{22}^{\mathrm{T}}L_{21}\right)\Delta_q(k)\right)^{\mathrm{T}}\Big)\\ &\quad=\mathcal{R}\Big(\left(\left(U_{12}^{\mathrm{T}}L_{12}+U_{22}^{\mathrm{T}}L_{22}\right)\Delta_q(k+q)\right)^{\mathrm{T}}\Big)\\ &\quad=\mathcal{R}\left(x^{\mathrm{T}}(k+q\colon k-q+\ell)\right).\end{aligned}\tag{65}$$

Next, note that (62) has $2pq-n$ rows, where $2pq-n\geq n$ by (31) of Theorem 1. Rewriting (55) we have

Multiplying both sides of (66) by $+\left(U_{12}^{\mathrm{T}}L_{11}+U_{22}^{\mathrm{T}}L_{21}\right)$, taking the upper blocks, and using (56) we have

$$\begin{aligned}&\left(U_{12}^{\mathrm{T}}L_{11}+U_{22}^{\mathrm{T}}L_{21}\right)\Delta_q(k)=\left(U_{12}^{\mathrm{T}}L_{11}+U_{22}^{\mathrm{T}}L_{21}\right)\\ &\quad\times\begin{bmatrix}\left(L_{11}-L_{12}L_{22}^{-1}L_{21}\right)^{-1}U_{11}S_{11} & \\ & 0\\ -L_{11}^{-1}L_{21}\left(L_{22}-L_{21}L_{11}^{-1}L_{12}\right)^{-1}U_{21}S_{11} & \end{bmatrix}V^{\mathrm{T}}M^{-1}\\ &\quad=\begin{bmatrix}U_lS_lV_l^{\mathrm{T}} & 0\end{bmatrix}V^{\mathrm{T}}M^{-1}=U_l\begin{bmatrix}S_lV_l^{\mathrm{T}} & 0\end{bmatrix}V^{\mathrm{T}}M^{-1}.\end{aligned}\tag{67}$$

Multiplying both sides of (66) by $-(U_{12}^{\mathrm{T}}L_{12}+U_{22}^{\mathrm{T}}L_{22})$, taking the lower blocks, and using (57) yields

$$\begin{aligned}
&-\big(U_{12}^{\mathrm{T}}L_{12}+U_{22}^{\mathrm{T}}L_{22}\big)\Delta_q(k+q)\\
&\quad=\big(U_{12}^{\mathrm{T}}L_{12}+U_{22}^{\mathrm{T}}L_{22}\big)\\
&\qquad\times\begin{bmatrix} L_{22}^{-1}L_{21}\big(L_{11}-L_{12}L_{22}^{-1}L_{21}\big)^{-1}U_{11}S_{11} & 0\\ -\big(L_{22}-L_{21}L_{11}^{-1}L_{12}\big)^{-1}U_{21}S_{11} & \end{bmatrix}V^{\mathrm{T}}M^{-1}\\
&\quad=\big[\,U_rS_rV_r^{\mathrm{T}}\quad 0\,\big]V^{\mathrm{T}}M^{-1}=U_r\big[\,S_rV_r^{\mathrm{T}}\quad 0\,\big]V^{\mathrm{T}}M^{-1}.
\end{aligned}\tag{68}$$

Using (17), (68), and (65) we have

$$\begin{aligned}
&\mathcal{R}\Big(\big(U_l^{\mathrm{T}}\big(U_{12}^{\mathrm{T}}L_{11}+U_{22}^{\mathrm{T}}L_{21}\big)\Delta_q(k)\big)^{\mathrm{T}}\Big)\\
&\quad\subset\mathcal{R}\Big(\big(\big(U_{12}^{\mathrm{T}}L_{11}+U_{22}^{\mathrm{T}}L_{21}\big)\Delta_q(k)\big)^{\mathrm{T}}\Big)\\
&\quad=\mathcal{R}\big(x^{\mathrm{T}}(k+q\colon k+\ell-q)\big),
\end{aligned}\tag{69}$$

$$\begin{aligned}
&\mathcal{R}\Big(\big(U_r^{\mathrm{T}}\big(U_{12}^{\mathrm{T}}L_{12}+U_{22}^{\mathrm{T}}L_{22}\big)\Delta_q(k+q)\big)^{\mathrm{T}}\Big)\\
&\quad\subset\mathcal{R}\Big(\big(\big(U_{12}^{\mathrm{T}}L_{12}+U_{22}^{\mathrm{T}}L_{22}\big)\Delta_q(k+q)\big)^{\mathrm{T}}\Big)\\
&\quad=\mathcal{R}\big(x^{\mathrm{T}}(k+q\colon k+\ell-q)\big).
\end{aligned}\tag{70}$$

Also using (67) and (68),

$$\begin{aligned}
&\operatorname{rank}U_l{}^{\mathrm{T}}\big(U_{12}^{\mathrm{T}}L_{11}+U_{22}^{\mathrm{T}}L_{21}\big)\Delta_q(k)\\
&\quad=\operatorname{rank}\big[\,S_lV_l^{\mathrm{T}}\quad 0\,\big]V^{\mathrm{T}}M^{-1}\\
&\quad=n\\
&\quad=\operatorname{rank}x(k+q\colon k+\ell-q),
\end{aligned}\tag{71}$$

$$\begin{aligned}
&\operatorname{rank}U_r{}^{\mathrm{T}}\big(U_{12}^{\mathrm{T}}L_{12}+U_{22}^{\mathrm{T}}L_{22}\big)\Delta_q(k+q)\\
&\quad=\operatorname{rank}\big[\,S_rV_r^{\mathrm{T}}\quad 0\,\big]V^{\mathrm{T}}M^{-1}\\
&\quad=n\\
&\quad=\operatorname{rank}x(k+q\colon k+\ell-q).
\end{aligned}\tag{72}$$

Thus

$$\begin{aligned}
&\mathcal{R}\Big(\big(U_l^{\mathrm{T}}\big(U_{12}^{\mathrm{T}}L_{11}+U_{22}^{\mathrm{T}}L_{21}\big)\Delta_q(k)\big)^{\mathrm{T}}\Big)\\
&\quad=\mathcal{R}\big(x^{\mathrm{T}}(k+q\colon k+\ell-q)\big),
\end{aligned}\tag{73}$$

$$\begin{aligned}
&\mathcal{R}\Big(\big(U_r^{\mathrm{T}}\big(U_{12}^{\mathrm{T}}L_{12}+U_{22}^{\mathrm{T}}L_{22}\big)\Delta_q(k+q)\big)^{\mathrm{T}}\Big)\\
&\quad=\mathcal{R}\big(x^{\mathrm{T}}(k+q\colon k+\ell-q)\big),
\end{aligned}\tag{74}$$

and thus there exist non-singular $T_l, T_r\in\mathbb{R}^{n\times n}$ such that

$$\begin{aligned}
x(k+q\colon k+\ell-q)&=T_lU_l^{\mathrm{T}}\big(U_{12}^{\mathrm{T}}L_{11}+U_{22}^{\mathrm{T}}L_{21}\big)\Delta_q(k)\\
&=-T_rU_r^{\mathrm{T}}\big(U_{12}^{\mathrm{T}}L_{12}+U_{22}^{\mathrm{T}}L_{22}\big)\Delta_q(k+q).
\end{aligned}\tag{75}$$

Proposition 2 shows that (54) is satisfied with $M_1=U_l^{\mathrm{T}}(U_{12}^{\mathrm{T}}L_{11}+U_{22}^{\mathrm{T}}L_{21})$ and $M_2=-U_r^{\mathrm{T}}U_{12}^{\mathrm{T}}L_{12}+U_{22}^{\mathrm{T}}L_{22})$. We take $L=I_{2q(p+\sigma)}$ and $M=I_{\ell-2q+1}$ in the numerical examples that follow. Assumption (58) is satisfied for $L=I_{2q(p+\sigma)}$. Different choices for L and M select different bases for the state sequence.

Another method for computing an approximation of the intersection of the row spaces of $\Delta_q(k)$ and $\Delta_q(k+q)$ is to compute the first n canonical vectors (Van Overschee and De Moor 1996) as follows.

Proposition 3: *Assume* (i)–(vi) *of Theorem* 1 *are satisfied. Then*

$$\begin{aligned}
&x(k+q\colon k+\ell-q)\\
&\quad=\frac{1}{2}\big(x_{cl}(k+q\colon k+\ell-q)+x_{cr}(k+q\colon k+\ell-q)\big),
\end{aligned}\tag{76}$$

where

$$x_{cl}(k+q\colon k+\ell-q)=U_1^{\mathrm{T}}\Big(\hat{\Delta}_q(k)\hat{\Delta}_q^{\mathrm{T}}(k)\Big)^{-1/2}\hat{\Delta}_q(k),\tag{77}$$

$$\begin{aligned}
&x_{cr}(k+q\colon k+\ell-q)\\
&\quad=V_1^{\mathrm{T}}\Big(\hat{\Delta}_q(k+q)\hat{\Delta}_q^{\mathrm{T}}(k+q)\Big)^{-1/2}\hat{\Delta}_q(k+q),
\end{aligned}\tag{78}$$

$$U_c=\big[\,U_1\quad U_2\,\big],\tag{79}$$

$$V_c=\big[\,V_1\quad V_2\,\big],\tag{80}$$

and U, S, and V are defined through the singular value decomposition

$$\begin{aligned}
U_cS_cV_c^{\mathrm{T}}=&\Big(\hat{\Delta}_q(k)\hat{\Delta}_q^{\mathrm{T}}(k)\Big)^{-1/2}\Big(\hat{\Delta}_q(k)\hat{\Delta}_q^{\mathrm{T}}(k+q)\Big)\\
&\Big(\hat{\Delta}_q(k+q)\hat{\Delta}_q^{\mathrm{T}}(k+q)\Big)^{-1/2},
\end{aligned}\tag{81}$$

where $U_c\in\mathbb{R}^{q\sigma+n\times q\sigma+n}$, $S_c\in\mathbb{R}^{q\sigma+n\times q\sigma+n}$, $V_c\in\mathbb{R}^{q\sigma+n\times q\sigma+n}$, $U_1\in\mathbb{R}^{q\sigma+n\times n}$, $U_2\in\mathbb{R}^{q\sigma+n\times q\sigma}$, $V_1\in\mathbb{R}^{q\sigma+n\times n}$, $V_2\in\mathbb{R}^{q\sigma+n\times q\sigma}$, and $\hat{\Delta}_q(k)\in\mathbb{R}^{q\sigma+n\times\ell-2q+1}$ and $\hat{\Delta}_q(k+q)\in\mathbb{R}^{q\sigma+n\times\ell-2q+1}$ are given by

$$\hat{\Delta}_q(k)=U_{\Delta_q(k)1}^{\mathrm{T}}\Delta_q(k),\tag{82}$$

$$\hat{\Delta}_q(k+q)=U_{\Delta_q(k+q)1}^{\mathrm{T}}\Delta_q(k+q),\tag{83}$$

where $U_{\Delta_q(k)1}\in\mathbb{R}^{q\sigma+n\times q(\sigma+p)}$, and $U_{\Delta_q(k+q)1}\in\mathbb{R}^{q\sigma+n\times q(\sigma+p)}$ are defined through the singular value decompositions

$$\begin{bmatrix} U_{\Delta_q(k)1} & U_{\Delta_q(k)2} \end{bmatrix} \begin{bmatrix} S_{\Delta_q(k)1} & 0 \\ 0 & 0 \end{bmatrix} \begin{bmatrix} V^{\mathrm{T}}_{\Delta_q(k)1} \\ V^{\mathrm{T}}_{\Delta_q(k)2} \end{bmatrix} = U_{\Delta_q(k)1} S_{\Delta_q(k)1} V^{\mathrm{T}}_{\Delta_q(k)1} = \Delta_q(k) \tag{84}$$

$$\begin{bmatrix} U_{\Delta_q(k+q)1} & U_{\Delta_q(k+q)2} \end{bmatrix} \begin{bmatrix} S_{\Delta_q(k+q)1} & 0 \\ 0 & 0 \end{bmatrix} \begin{bmatrix} V^{\mathrm{T}}_{\Delta_q(k+q)1} \\ V^{\mathrm{T}}_{\Delta_q(k+q)2} \end{bmatrix} = U_{\Delta_q(k+q)1} S_{\Delta_q(k+q)1} V^{\mathrm{T}}_{\Delta_q(k+q)1} = \Delta_q(k+q). \tag{85}$$

In Proposition 3 we had to find smaller, full rank, approximations $\hat{\Delta}_q(k)$ and $\hat{\Delta}_q(k+q)$ of the data matrices $\Delta_q(k)$ and $\Delta_q(k+q)$ in (84) and (85) and then compute the canonical vectors in (81). In the examples that follow, the method of Proposition 2 is used to estimate the state sequence.

4. Noise effects

Since $w(k)$ and $v(k)$ are present in real systems, we apply Theorem 1 and Proposition 2 without Assumption (ii).

The problem of rank determination is central to estimating the order of the unknown system. The presence of $w(k)$ and $v(k)$ will generally increase the rank of

$$L \begin{bmatrix} \Delta_q(k) \\ \Delta_q(k+q) \end{bmatrix} M.$$

For computational purposes, we use the following heuristic technique to estimate the rank of a matrix in the presence of noise. For $P \in \mathbb{R}^{2q(p+\sigma)\times \ell-2q+1}$, consider the singular value decomposition given by

$$P \triangleq USV^{\mathrm{T}}. \tag{86}$$

Let $s \in \mathbb{R}^{\min(2q(p+\sigma),\, \ell-2q+1)-2q\sigma}$, where, for $i = 1, \ldots, \min(2q(p+\sigma), \ell-2q+1) - 2q\sigma$,

$$s_i \triangleq \begin{cases} \dfrac{S(i,i)}{S(i+1,i+1)}, & \text{if } 2q\sigma \le i < \min(2q(p+\sigma), \ \ell-2q+1) \text{ and } S(i+1,i+1) \ne 0, \\ 0, & \text{else.} \end{cases} \tag{87}$$

Then we define

$$\operatorname{numrank} P \triangleq \arg\max s_i. \tag{88}$$

In the zero noise case

$$\operatorname{rank} L \begin{bmatrix} \Delta_q(k) \\ \Delta_q(k+q) \end{bmatrix} M \ge 2q\sigma,$$

so we have defined s_i to be zero for $i < 2q\sigma$.

Referring to (33) and (59), we approximate n and $x(k+q\colon k+\ell-q)$ by

$$\hat{n} \triangleq \operatorname{numrank}\left(L \begin{bmatrix} \Delta_q(k) \\ \Delta_q(k+q) \end{bmatrix} M \right) - 2q\sigma, \tag{89}$$

$$\hat{x}(k+q\colon k+\ell-q) \triangleq \tfrac{1}{2}\big(x_r(k+q\colon k+\ell-q) + \hat{x}_l(k+q\colon k+\ell-q)\big), \tag{90}$$

where

$$\hat{x}_r(k+q\colon k+\ell-q) \triangleq U_r^{\mathrm{T}}\big(U_{12}^{\mathrm{T}} L_{11} + U_{22}^{\mathrm{T}} L_{21}\big)\Delta_q(k), \tag{91}$$

$$\hat{x}_l(k+q\colon k+\ell-q) \triangleq -U_l^{\mathrm{T}}\big(U_{12}^{\mathrm{T}} L_{12} + U_{22}^{\mathrm{T}} L_{22}\big)\Delta_q(k+q), \tag{92}$$

and we have arbitrarily set $T = I$ in (59) to obtain (90). $T \ne I$ can be used to select a different basis for the state sequence. We have also suppressed the dependence on the time step k in $\hat{n}$ and s.

The presence of noise causes the row space of $\hat{x}_r(k+q\colon k+\ell-q)$ to be different from the row space of $\hat{x}_l(k+q\colon k+\ell-q)$. We use the mismatch between the row spaces of these two matrices to quantify the effect of noise, unmodelled non-linearities, and other model fit errors. To quantify this error, we use the principal angles between the two subspaces (see page 25 of Van Overschee and De Moor (1996). Define the singular value decomposition

$$\big(\hat{x}_r\hat{x}_r^{\mathrm{T}}\big)^{-1/2}\hat{x}_r\hat{x}_l^{\mathrm{T}}\big(\hat{x}_l\hat{x}_l^{\mathrm{T}}\big)^{-1/2} = U_{rl}S_{rl}V_{rl}^{\mathrm{T}}. \tag{93}$$

Then the principal cosines are the diagonal entries of S_{rl}, and the vector of principal angles $\alpha \in \mathbb{R}^{\hat{n}}$ is defined as

$$\alpha \triangleq \arccos(\operatorname{diag}(S_{rl})). \tag{94}$$

If the row spaces of $\hat{x}_r(k+q\colon k+\ell-q)$ and $\hat{x}_l(k+q\colon k+\ell-q)$ are equal, then the angles between them are zero. If the principal angles are small, then the two spaces are close to each other, whereas if the principal angles are large, then the two spaces are not.

6. Coefficient estimation

Now that we have the estimate $\hat{x}(k+q\colon k+\ell-q) \in \mathbb{R}^{n\times\ell-2q+1}$ given in (90) of the state sequence $x(k+q\colon k+\ell-q)$ we proceed to estimate A, B_1, B_2, C, D_1, and D_2 as well as the covariance matrices $Q \triangleq \mathcal{E}[w(k)w(k)^{\mathrm{T}}]$, $R \triangleq \mathcal{E}[v(k)v(k)^{\mathrm{T}}]$, and the correlation matrix E. Consider the cost function

$$J(\hat{A},\hat{B}_1,\hat{B}_2,\hat{C},\hat{D}_1,\hat{D}_2) \triangleq \left\| \begin{bmatrix} \hat{x}(k+q+1\colon k+\ell-q) \\ y(k+q\colon k+\ell-q-1) \end{bmatrix} - \begin{bmatrix} \hat{A} & \hat{B}_1 & 0 & \hat{B}_2 \\ \hat{C} & 0 & \hat{D}_1 & \hat{D}_2 \end{bmatrix} \begin{bmatrix} \hat{x}(k+q\colon k+\ell-q-1) \\ z(k+q\colon k+\ell-q-1) \end{bmatrix} \right\|_{\mathrm{F}}, \tag{95}$$

which can be written as

$$J^2(\hat{A},\hat{B}_1,\hat{B}_2,\hat{C},\hat{D}_1,\hat{D}_2) = J_1^2(\hat{A},\hat{B}_1,\hat{B}_2) + J_2^2(\hat{C},\hat{D}_1,\hat{D}_2),$$

where

$$J_1(\hat{A},\hat{B}_1,\hat{B}_2) \triangleq \left\| \hat{x}(k+q+1\colon k+\ell-q) - \begin{bmatrix} \hat{A} & \hat{B}_1 & \hat{B}_2 \end{bmatrix} R_1(k+q\colon k+\ell-q-1) \right\|_{\mathrm{F}},$$

$$J_2(\hat{C},\hat{D}_1,\hat{D}_2) \triangleq \left\| y(k+q\colon k+\ell-q-1) - \begin{bmatrix} \hat{C} & \hat{D}_1 & \hat{D}_2 \end{bmatrix} R_2(k+q\colon k+\ell-q-1) \right\|_{\mathrm{F}},$$

$\|\cdot\|_{\mathrm{F}}$ is the Frobenius matrix norm, and

$$R_1(k) \triangleq \begin{bmatrix} \hat{x}(k) \\ f(k) \\ h(k) \end{bmatrix}, \quad R_2(k) \triangleq \begin{bmatrix} \hat{x}(k) \\ g(k) \\ h(k) \end{bmatrix}.$$

Proposition 4: *The matrices*

$$\begin{bmatrix} \hat{A} & \hat{B}_1 & \hat{B}_2 \end{bmatrix} \triangleq \hat{x}(k+q+1\colon k+\ell-q) \times R_1(k+q\colon k+\ell-q-1)^{+}, \tag{96}$$

$$\begin{bmatrix} \hat{C} & \hat{D}_1 & \hat{D}_2 \end{bmatrix} \triangleq y(k+q\colon k+\ell-q-1) \times R_2(k+q\colon k+\ell-q-1)^{+} \tag{97}$$

minimize J_1 and J_2.

In practice, the generalized inverses in (96) and (97) can often be replaced by right inverses.

Proposition 5: *Let $\hat{A}$, $\hat{B}_1$, $\hat{B}_2$, $\hat{C}$, $\hat{D}_1$, and $\hat{D}_2$ be given by* (96) *and* (97). *Then the covariance of the residuals of* (95) *is given by*

$$\Sigma \triangleq \begin{bmatrix} \Sigma_{11} & \Sigma_{12} \\ \Sigma_{12}^{\mathrm{T}} & \Sigma_{22} \end{bmatrix}.$$

The corresponding estimates of E, Q, and R are

$$\hat{Q} \triangleq \Sigma_{11}, \tag{98}$$

$$\hat{E} \triangleq \Sigma_{21}\Sigma_{11}^{-1}, \tag{99}$$

$$\hat{R} \triangleq \Sigma_{22} - \Sigma_{21}\Sigma_{11}^{-1}\Sigma_{21}^{\mathrm{T}}, \tag{100}$$

where

$$\Sigma_{11} \triangleq \hat{x}(k+q+1\colon k+\ell-q)\Pi^{\perp}_{R_1(k+q\colon k+\ell-q-1)}\hat{x}^{\mathrm{T}} \times (k+q+1\colon k+\ell-q), \tag{101}$$

$$\Sigma_{21} \triangleq y(k+q\colon k+\ell-q-1)\big(I - \Pi_{R_1(k+q\colon k+\ell-q-1)} - \Pi_{R_2(k+q\colon k+\ell-q-1)} + \Pi_{R_1(k+q\colon k+\ell-q-1)} \times \Pi_{R_2(k+q\colon k+\ell-q-1)}\big)\hat{x}^{\mathrm{T}}(k+q+1\colon k+\ell-q), \tag{102}$$

$$\Sigma_{22} \triangleq y(k+q\colon k+\ell-q-1)\Pi^{\perp}_{R_2(k+q\colon k+\ell-q-1)}y^{\mathrm{T}} \times (k+q\colon k+\ell-q-1). \tag{103}$$

6. The algorithm

Here we summarize the steps in the non-linear subspace identification algorithm.

(1) Collect input–output data, and choose the window length q. The length of data to be used, ℓ, must be chosen less than or equal to the number of input–output data pairs available.
(2) Select the memory depth b and basis functions $f_i(k,u(k-b\colon k),y(k-b\colon k))$, $g_i(k,u(k-b\colon k),y(k-b\colon k-1))$, and $h_i(k,u(k-b\colon k), y(k-b\colon k-1))$ to model the system.
(3) Construct $\Delta_q(k)$ and $\Delta_q(k+q)$ as in (30).
(4) Select weighting matrices L and M, where M is non-singular, and L is block-invertible, i.e., L_{11}, L_{22}, $L_{11}-L_{12}L_{22}^{-1}L_{21}$, and $L_{22}-L_{21}L_{11}^{-1}L_{12}$ are non-singular.

(5) Calculate the primary singular value decomposition of

$$L\begin{bmatrix} \Delta_q(k) \\ \Delta_q(k+q) \end{bmatrix}M$$

in (55) and obtain $\hat{n}$ in (89) as well as U_{11}, U_{12}, U_{21}, U_{22}, and S_{11}.

(6) Calculate the singular value decompositions in (56) and (57) and obtain U_l and U_r.

(7) Estimate the state matrix $\hat{x}(k+q : k+\ell-q)$ in (90).

(8) Estimate the system matrices $\hat{A}$, $\hat{B}_1$, $\hat{B}_2$, $\hat{C}$, $\hat{D}_1$, and $\hat{D}_2$ in (96) and (97). Estimate $\hat{E}$ and the noise covariance matrices $\hat{Q}$ and $\hat{R}$ in (98), (99), and (100).

7. Examples

In this section the non-linear subspace identification algorithm is applied to several non-linear systems. The validation error is defined by

$$e \triangleq \frac{\|y(1:\ell) - \hat{y}(1:\ell)\|_{\mathrm{F}}}{\|y(1:\ell)\|_{\mathrm{F}}}, \tag{104}$$

where $\hat{y}$ is the output predicted by the identified model. For each example $L = I_{2q(p+\sigma)}$ and $M = I_{\ell-2q+1}$.

The coefficients of the identified model are not reported in the examples that follow since they can be difficult to compare to the coefficients in the original system. In the case where the original system does not fall in the model class, see § 7.2–7.4, direct comparison of coefficients is not suitable. In the case where the system is a member of the model class, see § 7.1, some manipulation may be required to set the basis for the state sequence, as well as manipulating the input coefficient values relative to the non-linear basis function coefficients. We present the validation error (104) as a useful tool for comparing the identified model and the system under study that has utility beyond the comparison of identified models to simulated systems to the comparison of identified models and measured data.

In the plots that follow, the variable t is related to the discrete variable k as $\tau k = t$. Where data from a continuous time system and a discrete time system are displayed on the same plot, the continuous time signal has been sampled at the same points as the discrete time data.

7.1. *Noise statistics example*

Here we examine in simulation the effects of varying the noise level. We simulate the single-input, single-output, four-state Hammerstein system

$$x(k+1) = \begin{bmatrix} 0 & 0 & 0.495 & 0.495 \\ 0.99 & 0 & 0 & 0 \\ 0 & 0.99 & 0 & 0 \\ 0 & 0 & 0.99 & 0 \end{bmatrix} x(k) + \begin{bmatrix} 1 & 0 \\ 0 & 1 \\ 0 & 0 \\ 0 & 0 \end{bmatrix}\begin{bmatrix} u(k) \\ u(k)^2 \end{bmatrix} \tag{105}$$

$$y(k) = \begin{bmatrix} 0 & 0 & 0 & 1 \end{bmatrix} x(k) + v(k). \tag{106}$$

We take $h = \begin{bmatrix} u & u^2 & u^3 \end{bmatrix}^{\mathrm{T}}$, $q = 2^4 = 16$, and $\ell = 2^{10} = 1024$. We take our input sequence u to be a realization of a zero mean unit variance normally distributed random variable. We add zero mean normally distributed measurement noise to the output, and adjust the signal to noise ratio for each run by changing the variance of the measurement noise, where we define the signal to noise ratio as

$$\frac{S}{N} \triangleq \frac{\|y - v\|}{\|v\|}. \tag{107}$$

We simulate twenty signal to noise ratios, logarithmically spaced from 0.01 to 1000. We plot the singular values in figure 5 and the principal angles in figure 6. We plot the true and estimate output noise variance in figure 7. As we increase the variance of the noise, we see that the ratios of singular values become less indicative of the order of the system and the principal angles increase toward 90 degrees. The output noise covariance estimates improve as the variance of the noise sequence increases. This is because the output noise is dominating the response of the system and the covariance of the output. Also, since the data sequences are finite, the algorithm may attribute effects actually due to noise to the system.

7.2. *Planar articulated spacecraft*

We model the planar motion of two flexible bodies linked by a hinge. For simplicity, we model only the first flexure mode of each link. The equations of

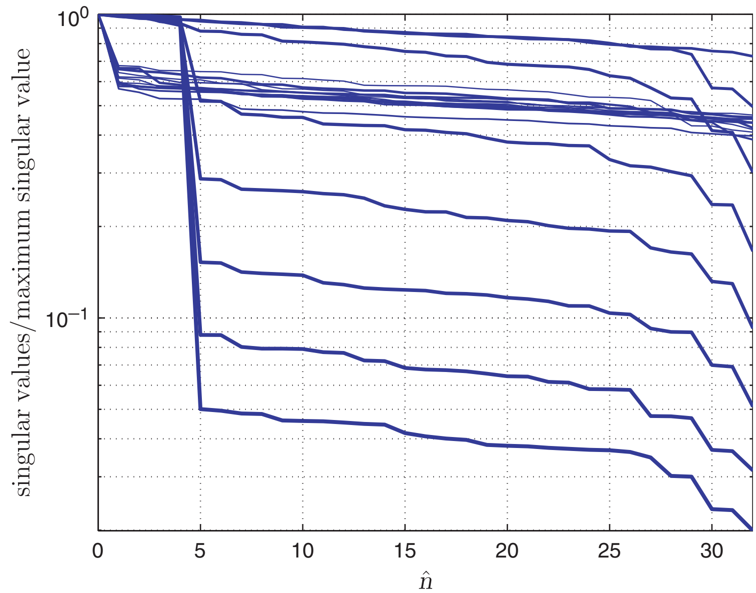

Figure 5. The singular values used to estimate $\hat{n}$ for each signal to noise ratio. The thickness of the line is proportional to S/N. As the noise level is decreased, the singular values become a good indicator of the system order.

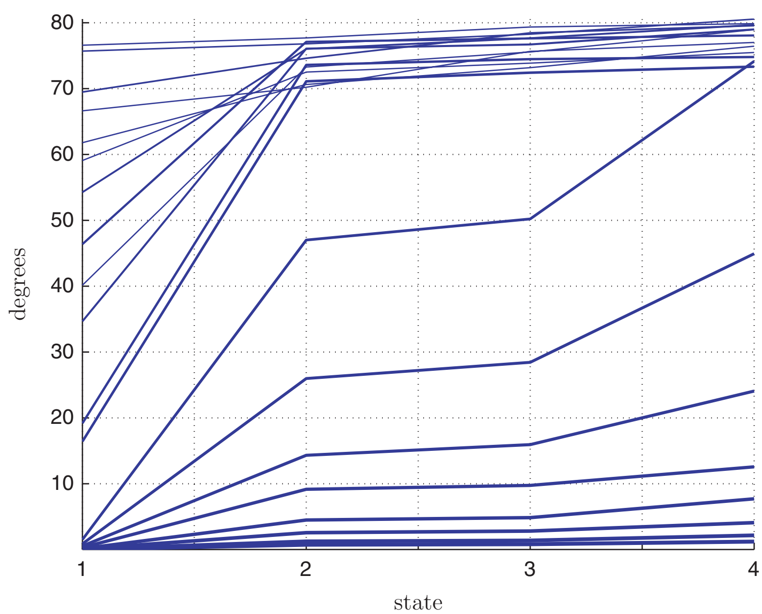

Figure 6. The principal angles are used to quantify the effect of noise for each signal to noise ratio. As the noise level increases, the subspaces become increasingly orthogonal. The thickness of the line is proportional to S/N.

motion are

$$\ddot{\theta}_1 = \frac{\sin\theta(\dot{\theta}_1^2\cos\theta - \lambda_2\dot{\theta}_2^2)}{-\lambda_1\lambda_2 + \cos^2\theta} + \sqrt{2}\delta_1\ddot{\zeta}_1 + u, \tag{108}$$

$$\ddot{\theta}_2 = -\frac{\sin\theta(\dot{\theta}_2^2\cos\theta - \lambda_1\dot{\theta}_1^2)}{-\lambda_1\lambda_2 + \cos^2\theta} + \sqrt{2}\delta_2\ddot{\zeta}_2 - u, \tag{109}$$

$$0 = \ddot{\zeta}_1 + 2c_1\omega_1\dot{\zeta}_1 + \omega_1^2\zeta_1 + \sqrt{2}\delta_1\ddot{\theta}_1, \tag{110}$$

$$0 = \ddot{\zeta}_2 + 2c_2\omega_2\dot{\zeta}_2 + \omega_2^2\zeta_2 + \sqrt{2}\delta_2\ddot{\theta}_2, \tag{111}$$

where $\lambda_1 = J_1/\eta$, $\lambda_2 = J_2/\eta$, $\eta = d_1 d_2 m$, $J_1 = I_1 + md_1^2$, $J_2 = I_2 + md_2^2$, $m = m_1 m_2/(m_1 + m_2)$ is the reduced mass, d_1 and d_2 are the distances from the hinge point to the center of mass of each body, m_1 and m_2 are the masses of the two bodies, $\theta = \theta_1 - \theta_2$ is the angle between the two bodies, θ_1 and θ_2 are the angular positions of the two bodies with respect to an inertial frame, ζ_1 and ζ_2 are the fundamental flexible modes of each body, ω_1 and ω_2 are the modal frequencies, δ_1 and δ_2

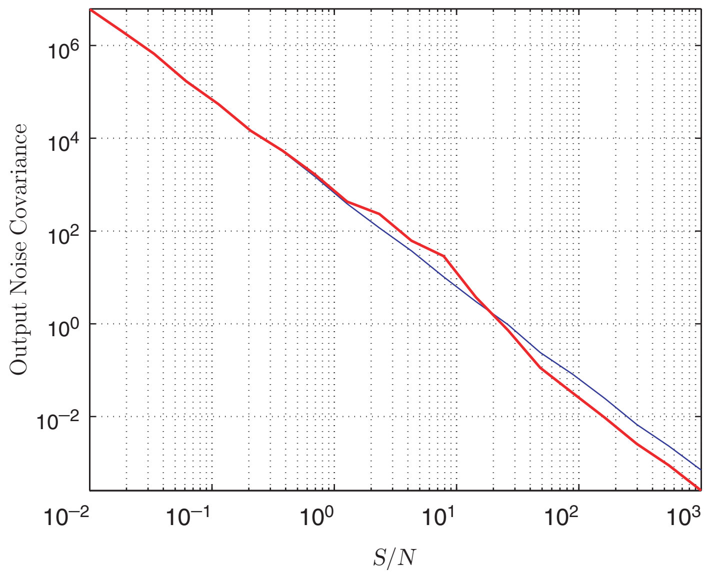

Figure 7. True (thin line) and estimated (thick line) noise covariance. The noise covariance estimate improves as the S/N degrades.

are the coupling coefficients, and u is the control torque applied between the two bodies. We can rewrite (7.5), (7.6), (7.7), and (7.8) as

$$\ddot{\theta}_1 = \frac{1}{1+2\delta_1^2}\left(\frac{\sin\theta\big(\dot{\theta}_1^2\cos\theta - \lambda_2\dot{\theta}_2^2\big)}{-\lambda_1\lambda_2+\cos^2\theta} - \sqrt{2}\delta_1\omega_1^2\zeta_1 - 2\sqrt{2}\delta_1 c_1\omega_1\dot{\zeta}_1 + u\right), \quad (112)$$

$$\ddot{\theta}_2 = \frac{1}{1+2\delta_1^2}\left(-\frac{\sin\theta\big(\dot{\theta}_2^2\cos\theta - \lambda_1\dot{\theta}_1^2\big)}{-\lambda_1\lambda_2+\cos^2\theta} - \sqrt{2}\delta_2\omega_2^2\zeta_2 - 2\sqrt{2}\delta_2 c_2\omega_2\dot{\zeta}_2 - u\right), \quad (113)$$

$$\ddot{\zeta}_1 = \frac{-1}{1+2\delta_1^2}\left(\frac{\sqrt{2}\delta_1\sin\theta\big(\dot{\theta}_1^2\cos\theta - \lambda_2\dot{\theta}_2^2\big)}{-\lambda_1\lambda_2+\cos^2\theta} + \omega_1^2\zeta_1 + 2c_1\omega_1\dot{\zeta}_1 + \sqrt{2}\delta_1 u\right), \quad (114)$$

$$\ddot{\zeta}_2 = \frac{-1}{1+2\delta_2^2}\left(-\frac{\sqrt{2}\delta_2\sin\theta\big(\dot{\theta}_2^2\cos\theta - \lambda_1\dot{\theta}_1^2\big)}{-\lambda_1\lambda_2+\cos^2\theta} + \omega_2^2\zeta_1 + 2c_2\omega_2\dot{\zeta}_2 + \sqrt{2}\delta_2 u\right). \quad (115)$$

Since $\lambda_1\lambda_2 > 1$ these equations do not have a singularity. For the experiment, the control signal u is a realization of a zero mean, unit variance random variable for the first 25 seconds, and zero after 25 seconds, when we observe the system free response. We measure $\ell = 2000$ data points with sampling rate $1/\tau = 20\,\text{Hz}$. We take measurements of θ_1, θ_2, $\dot{\theta}_1$, and $\dot{\theta}_2$, and set

$$z(k) = h(k) = \begin{bmatrix} u(k-1) \\ \dot{\theta}_1^2(k-1)\sin(\theta_1(k-1)-\theta_2(k-1)) \\ \dot{\theta}_2^2(k-1)\sin(\theta_1(k-1)-\theta_2(k-1)) \\ \dot{\theta}_1^2(k-1)\sin 2(\theta_1(k-1)-\theta_2(k-1)) \\ \dot{\theta}_2^2(k-1)\sin 2(\theta_1(k-1)-\theta_2(k-1)) \end{bmatrix}, \quad (116)$$

a function of delayed data, with the nonlinearities periodic in θ. We obtain a fourth order model and plot the validation data in figure 8. The validation error is $e = 0.0025$. The frequency of the oscillations in $\dot{\theta}_1$ and $\dot{\theta}_2$ is closely matched.

7.3. *Forced Van der Pol oscillator*

Here we consider the system

$$\dot{x}_1 = x_2, \quad (117)$$

$$\dot{x}_2 = -\omega^2 x_1 + \epsilon\omega\big(1-\mu^2 x_1^2\big)x_2 + u \quad (118)$$

with $\omega = \epsilon = \mu = 1$. We excite this continuous-time system with a zero-order-held sequence of $\ell = 1000$ input samples with time interval $\tau = 0.05\,\text{s}$, and measure ℓ samples of both x_1 and x_2 with sampling rate $1/\tau = 20\,\text{Hz}$. Since the nonlinearities are functions of x_1 and x_2, we measure both signals and identify a discrete-time model. Inspired by the continuous-time

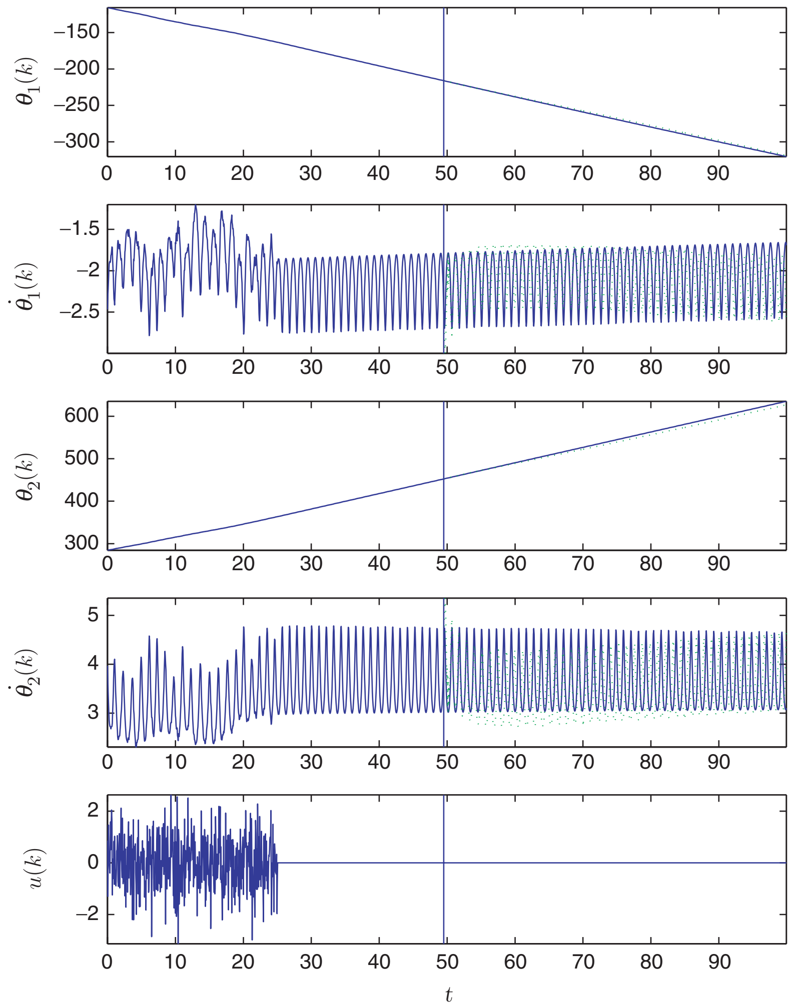

Figure 8. The time trace of measured and estimated variables. The vertical line indicates the end of the identification data set and the beginning of the validation data set. The solid line indicates the signal from the true continuous-time system. The dotted line indicates the signal from the identified discrete-time model.

system, we first choose

$$z(k) = h(k) = \begin{bmatrix} x_1(k) \\ x_2(k) \\ x_1^2(k)x_2(k) \\ u(k) \end{bmatrix} \tag{119}$$

and identify a discrete-time model. We then continue the input sequence as shown in figure 9 and measure outputs of both the true continuous-time system and the identified discrete-time model and compare the results. The validation error is $e = 0.0207$. See figure 9 and figure 10.

Without exploiting knowledge of the structure of the continuous-time system, we alternatively choose all polynomials up to third order as our basis functions, so that

$$z(k) = h(k) = \begin{bmatrix} 1 & x_1(k) & x_2(k) & u(k) \\ x_1(k)^2 & x_2(k)^2 & u(k)^2 & x_1(k)x_2(k) \\ x_2(k)u(k) & u(k)x_1(k) & x_1(k)^3 & x_2(k)^3 \\ u(k)^3 & x_1(k)^2x_2(k) & x_1(k)x_2(k)^2 & x_2(k)^2u(k) \\ x_2(k)u(k)^2 & u(k)^2x_1(k) & u(k)x_1(k)^2 & x_1(k)x_2(k)u(k) \end{bmatrix}^{\mathrm{T}}. \tag{120}$$

Using the same data as before, we identify a discrete-time model and compare the output of both the true continuous-time system and the identified discrete-time model. The validation error is $e = 0.0672$. See figure 11 and figure 12. Note that

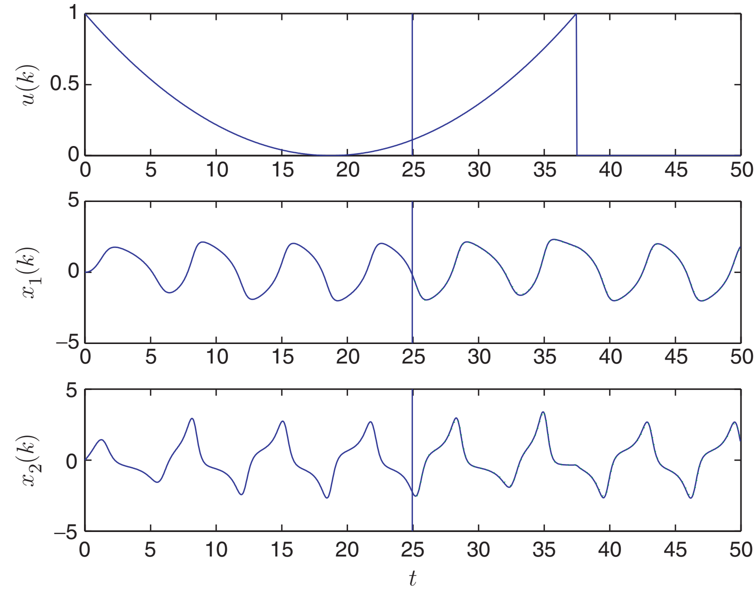

Figure 9. The time trace of measured and estimated variables of the forced Van der Pol oscillator with 4 basis functions. The vertical line indicates the end of the identification data set and the beginning of the validation data set. The solid line indicates the signal from the true continuous-time system. The dotted line indicates the signal from the identified discrete-time model.

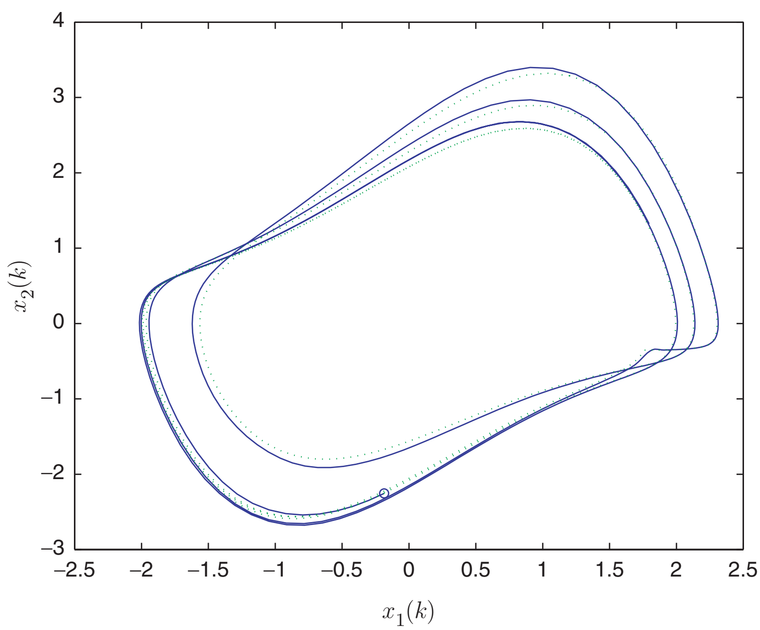

Figure 10. x_1 vs. x_2 validation signals for the forced Van der Pol oscillator with 4 basis functions. The solid line indicates the signal from the true continuous-time system. The dotted line indicates the signal from the identified discrete-time model.

even though we have increased the number of basis functions, the validation error has not decreased; in fact it increased by a factor of 3.5. While we increased the number of basis functions, and thus increased the ability of the identified system to match the identification data set, we have over-modelled the data. The estimated system output matches the true output well for the identification data set, but does not perform as well when applied to the validation data set. This effect can be reduced by using a larger data set, or a better set of basis functions, see Palanth *et al*. (2004).

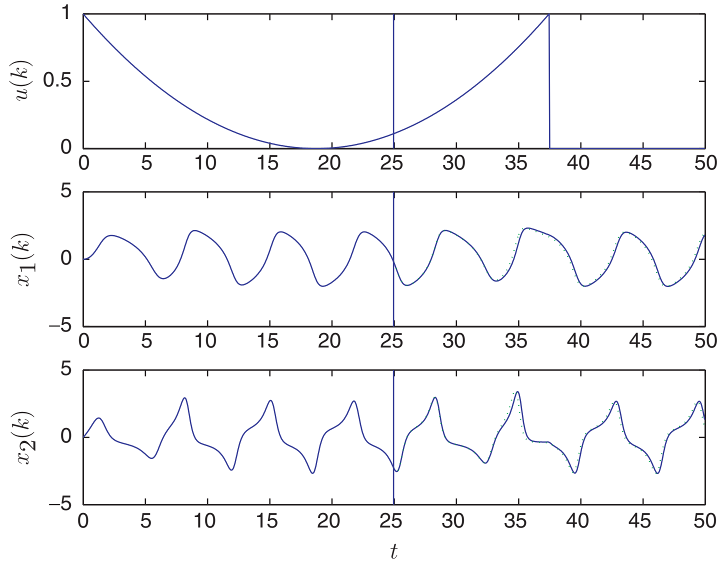

Figure 11. The time trace of measured and estimated variables of the forced Van der Pol oscillator with 20 basis functions. The vertical line indicates the end of the identification data set and the beginning of the validation data set. The solid line indicates the signal from the true continuous-time system. The dotted line indicates the signal from the identified discrete-time model.

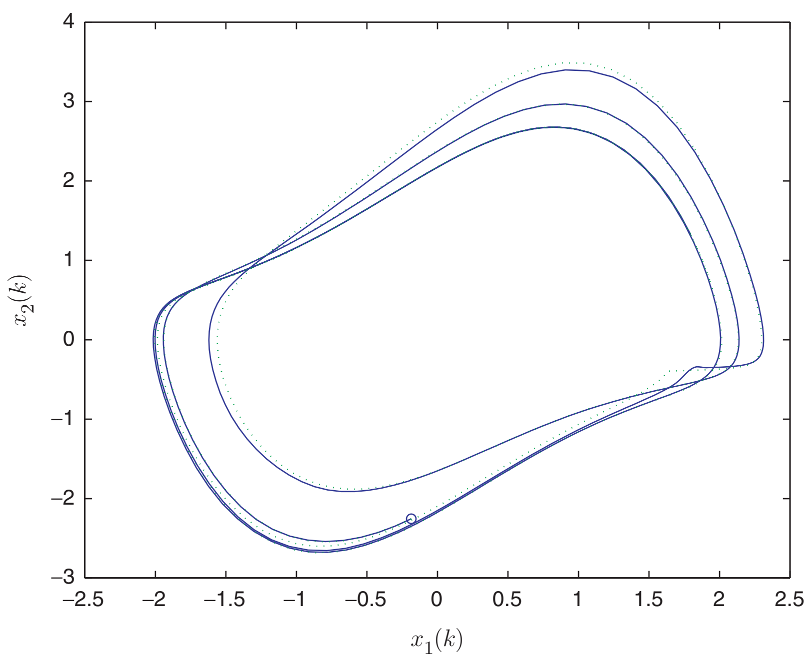

Figure 12. x_1 vs. x_2 validation signals for the forced Van der Pol oscillator with 20 basis functions. The solid line indicates the signal from the true continuous-time system. The dotted line indicates the signal from the identified discrete-time model.

7.4. *Elliptical limit cycle*

Here we consider the unforced system

$$\ddot{q} + \lambda\left(q^2 + \left(\frac{\dot{q}}{\omega}\right)^2 - a^2\right)\dot{q} + \omega^2 q = 0, \qquad (121)$$

with $\lambda = 2$, $a = 1$, $\omega = 2$. This system converges to a sinusoidal output with amplitude a and frequency ω. We rewrite this system with $x_1 = q$ and $x_2 = \dot{q}$ as

$$\dot{x}_1 = x_2, \qquad (122)$$

$$\dot{x}_2 = \lambda a^2 x_2 - \frac{\lambda}{\omega^2} x_2^3 - \lambda x_1^2 x_2 - \omega^2 x_1. \qquad (123)$$

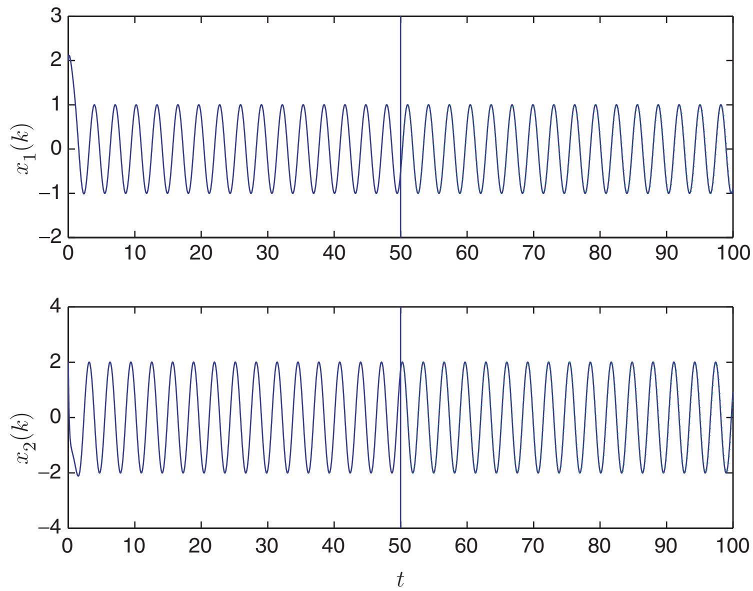

Figure 13. The time trace of measured and estimated variables of the Elliptical Limit Cycle with 4 basis functions. The vertical line indicates the end of the identification data set and the beginning of the validation data set. The solid line indicates the signal from the true continuous-time system. The dotted line indicates the signal from the estimated discrete-time system.

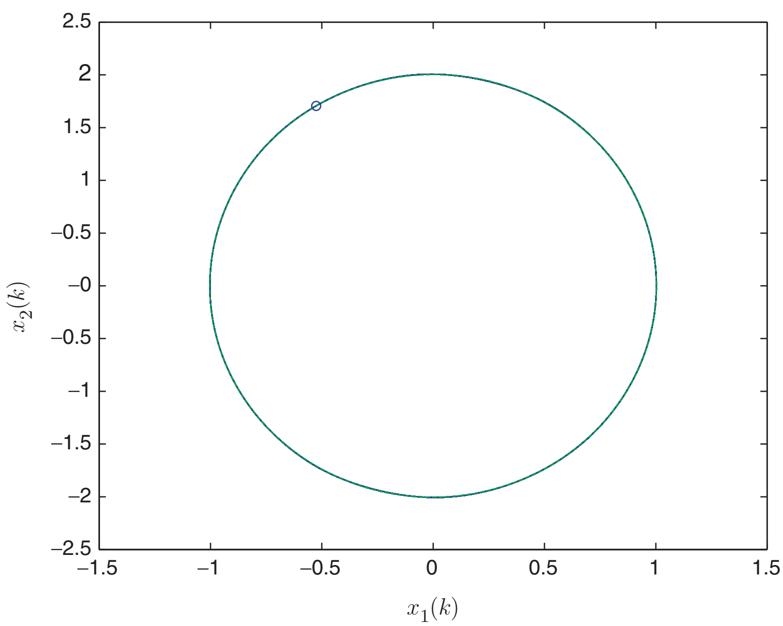

Figure 14. x_1 vs. x_2 validation signals for the Elliptical Limit Cycle with 4 basis functions. The solid line indicates the signal from the true continuous-time system. The dotted line indicates the signal from the estimated discrete-time system.

In this example there is no input to the system. We measure a zero-order held sequence of $\ell = 10000$ outputs with time interval $\tau = 0.01$ s. As with the previous example of the Van der Pol Oscillator, we assume access to both x_1 and x_2. Inspired by the continuous-time system we choose

$$z(k) = h(k) = \begin{bmatrix} x_1(k) \\ x_2(k) \\ x_1^2(k)x_2(k) \\ x_2^3(k) \end{bmatrix} \tag{124}$$

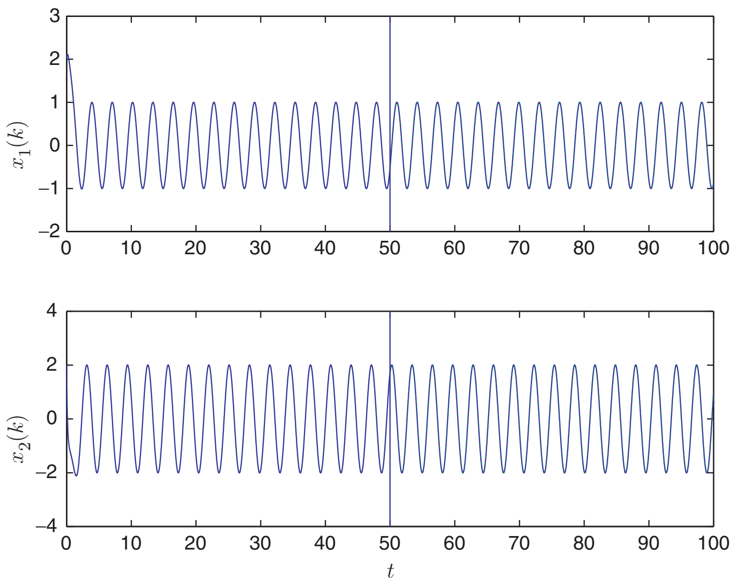

Figure 15. The time trace of measured and estimated variables of the Elliptical Limit Cycle with 10 basis functions. The vertical line indicates the end of the identification data set and the beginning of the validation data set. The solid line indicates the signal from the true continuous-time system. The dotted line indicates the signal from the estimated discrete-time system.

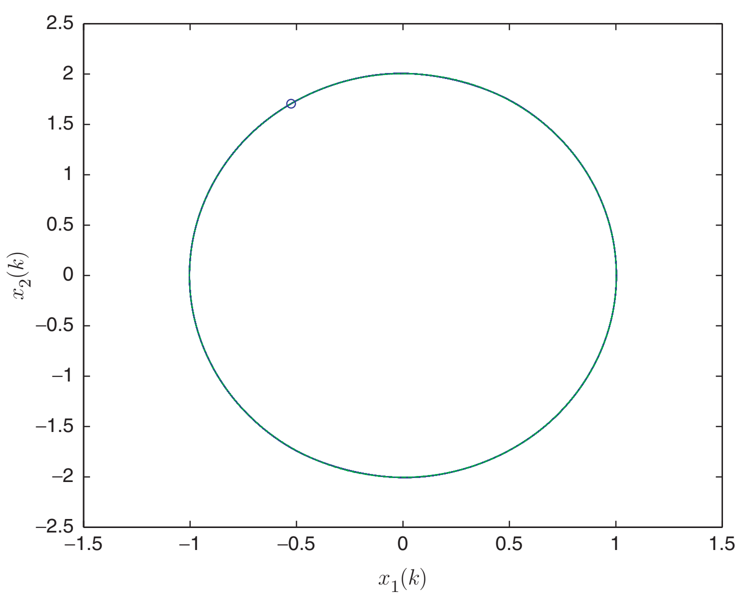

Figure 16. x_1 vs. x_2 validation signals for the Elliptical Limit Cycle with 10 basis functions. The solid line indicates the signal from the true continuous-time system. The dotted line indicates the signal from the estimated discrete-time system.

and obtain a validation error of $e = 0.0678$. See figure 13 and figure 14. Alternatively, we choose

$$z(k) = h(k) = \begin{bmatrix} 1 & x_1(k) & x_2(k) & x_1^2(k) \\ x_2^2(k) & x_1(k)x_2(k) & x_1^3(k) & x_2^3(k) \\ x_1^2(k)x_2(k) & x_1(k)x_2^2(k) & & \end{bmatrix}^{\mathrm{T}}, \tag{125}$$

the set of all polynomials up to third order in the outputs and obtained a validation error of $e = 0.0015$. See figure 15 and figure 16. Unlike the previous example, the validation error decreases as we increase the number of basis functions.

Next, we identify the system with only one measurement and increase the memory depth of the non-linear basis functions. Assuming access to only the position variable x_1 we include delayed outputs in our basis

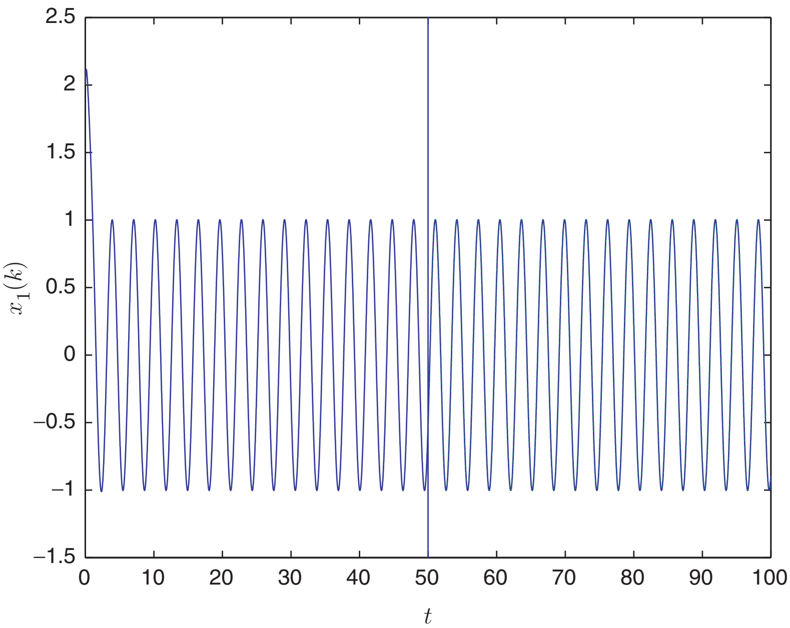

Figure 17. The time trace of measured and estimated variables of the Elliptical Limit Cycle with 10 basis functions and measurement of $x_1(k)$ only. The vertical line indicates the end of the identification data set and the beginning of the validation data set. The solid line indicates the signal from the true continuous-time system. The dotted line indicates the signal from the estimated discrete-time system.

functions by letting

$$f(k) = \begin{bmatrix} 1 & x_1(k-1) & x_1(k) \; x_1^2(k-1) \; x_1^2(k) \\ x_1(k-1)x_1(k) & x_1^3(k-1) & \\ x_1^3(k) & x_1^2(k-1)x_1(k) & x_1(k-1) \; x_1^2(k) \end{bmatrix}^{\mathrm{T}}. \tag{126}$$

See figure 17. While the error has increased substantially to $e = 0.0087$, it is still less than one percent. This example demonstrates how including functions of delayed data can allow identification of a system that would otherwise be difficult to identify.

8. Conclusion

We presented a subspace-based identification method for identifying non-linear time-varying systems that are nonlinear in measured data and linear in unmeasured states. Our approach is to rewrite the nonlinear identification problem as a linear identification problem by writing the system nonlinearities as a sum of known basis functions with unknown coefficients. We then applied the algorithm to several numerical examples. Future work will focus on experimental applications (Lacy and Bernstein 2002), extending the class of identifiable systems, and methods for basis function selection (Palanth *et al.* 2004).

Acknowledgements

Supported in part by NASA under GSRP NGT4-52421 and AFOSR under grant F49620-01-1-0094 and laboratory research initiative 00VS17COR.

References

H. Al-Duwaish and M. Nazmul Karim, "A new method for the identification of hammerstein model", *Automatica*, 33, pp. 1871–1875, 1997.

W. N. Anderson Jr and R. J. Duffin, "Series and parallel addition of matrices", *Journal of Mathematical Analysis and Applications*, 26, pp. 576–594, 1969.

E.-W. Bai, "An optimal two-stage identification algorithm for Hammerstein-Wiener nonlinear systems", *Automatica*, 34, pp. 333–338, 1998.

E.-W. Bai, "Identification of linear systems with hard input non-linearities of known structure", *Automatica*, 38, pp. 853–860, 2002.

D. Bauer, "Order estimation for subspace methods", *Automatica*, 37, pp. 1561–1573, 2001.

D. Bauer, M. Deistler and W. Scherrer, "Consistency and asymptotic normality of some subspace algorithms for systems without observed inputs", *Automatica*, 35, pp. 1243–1254, 1999.

D. Bauer and M. Jansson, "Analysis of the asymptotic properties of the moesp type of subspace algorithms", *Automatica*, 36, pp. 197–509, 2000.

D. Bauer and L. Ljung, "Some facts about the choice of weighting matrices in larimore type of subspace algorithms", *Automatica*, 38, pp. 763–773, 2002.

C. Blaurock, *Dynamod Users Manual*, Medford, MA: Midé Technology Corporation, 2003.

C.H. Chen and S.D. Fassois, "Maximum likelihood identification of stochastic Wiener-Hammerstein-type non-linear systems", *Mechanical Systems and Signal Processing*, 6, pp. 135–153, 1992.

M. Deistler, K. Peternell and W. Scherrer, "Consistency and relative efficiency of subspace methods", *Automatica*, 31, pp. 1865–1875, 1995.

W. Greblicki, "Nonparametric identification of Wiener systems", *IEEE Transactions on Information Theory*, 38, pp. 1487–1493, 1992.

W. Greblicki, "Nonparametric approach to Wiener system identification", *IEEE Transactions on Circuits and Systems – I: Fundamental Theory and Applications*, 44, pp. 538–545, 1997.

W. Greblicki and M. Pawlak, "Nonparametric identification of hammerstein systems", *IEEE Transactions on Information Theory*, 35, pp. 409–418, 1989.

H. Haverkamp and M. Verhaegen, *Subspace Model Identification Toolbox*, Systems and Control engineering Group, Delft University of Technology, 1997.

M. Jansson and B. Wahlberg, "On consistency of subspace methods for system identification", *Automatica*, 34, pp. 1507–1519, 1998.

R. Johansson, A. Robertsson, K. Nilsson and M. Verhaegen, "State-space system identification of robot manipulator dynamics", *Mechatronics*, 10, pp. 403–418, 2000.

R. Johansson, M. Verhaegen and C.T. Chou, "Stochastic theory of continuous-time state-space identification", *IEEE Transactions on Signal Processing*, 47, pp. 41–51, 1999.

J.-N. Juang, *Applied System Identification*, Englewood Cliffs, NJ: Prentice Hall, 1993.

T. Knudsen, "Consistency analysis of subspace identification methods based on a linear regression approach", *Automatica*, 37, pp. 81–89, 2001.

S.L. Lacy and D.S. Bernstein, "Nonlinear identification of an active vibration isolation strut", in *Proceedings of the Conference on Decision and Control*, Las Vegas, NV, 2002, pp. 4521–4526.

S.L. Lacy and D.S. Bernstein, "Identification of FIR wiener systems with unknown, non-invertible, polynomial nonlinearities", *International Journal of Control*, 76, pp. 1500–1507, 2003a.

S.L. Lacy and D.S. Bernstein, "Subspace identification with guaranteed stability using constrained optimization", *IEEE Transactions on Automatic Control*, 48, pp. 1259–1263, 2003b.

S.L. Lacy, R.S. Erwin and D.S. Bernstein, "Identification of Wiener systems with known noninvertible nonlinearities", *Journal of Dynamic Systems, Measurement, and Control*, 123, pp. 566–571, 2001.

W.E. Larimore, "Generalized canonical variate analysis of nonlinear systems", in *Proceedings of the 27th Conference on Decision and Control*, Austin, TX: IEEE, 1988, pp. 1720–1725.

W.E. Larimore, ADAPT_X *Users Manual*, McLean VA: Adaptics, Inc., 1999a.

W.E. Larimore, "Automated multivariable system identification and industrial applications", in *Proceedings of the American Control Conference*, San Diego, CA, 1999b, pp. 1148–1162.

W. Li and J. Qin, "Consistent dynamic PCA based on errors-in-variables subspace identification", *Process Control*, 11, pp. 661–678, 2001.

L. Ljung, *System Identification: Theory for the User*, Prentice Hall Information and System Sciences Series, 2nd ed., Upper Saddle River, NJ: Prentice Hall, 1999.

L. Ljung and T. McKelvey, "Subspace identification from closed loop data", *Signal Processing*, 52, pp. 209–215, 1996.

M. Lovera, T. Gustafsson and M. Verhaegen, "Recursive subspace identification of linear and non-linear Wiener state-space models", *Automatica*, 36, pp. 1639–1650, 2000.

M. Lovera, T. Parisini and M. Verhaegen, "Fault detection, a subspace identification approach", in *Proceedings of the 40th IEEE Conference on Decision and Control*, Orlando, FL, 2001, pp. 2275–2276.

MATLAB, *System Identification Toolbox*, Natick, MA: Mathworks, 2003.

T. McKelvey, H. Akçay and L. Ljung, "Subspace-based identification of infinite-dimensional multivariable systems from frequency-response data", *Automatica*, 32, pp. 885–902, 1996.

M. Moonen, B. De Moor, L. Vandenberghe and J. Vandewalle, "On- and off-line identification of linear state-space models", *International Journal of Control*, 49, pp. 219–232, 1989.

H. Palanth, J.B. Hoagg and D.S. Bernstein, "A selective refinement algorithm for nonlinear identification of systems with measured-input nonlinearities", in *Proceedings of the American Control Conference*, Boston, MA, 2004.

K. Peternell, W. Scherrer and M. Deistler, "Statistical analysis of novel subspace identification methods", *Signal Processing*, 52, pp. 161–177, 1996.

R. Pintelon, "Frequency domain subspace system identification using non-parametric noise models", *Automatica*, 38, pp. 1295–1311, 2002.

R. Pintelon and J. Schoukens, *System Identification: A Frequency Domain Approach*, Piscataway, NJ: IEEE Press, 2001.

J. Schoukens, J.G. Nemeth, P. Crama, Y. Rolain and R. Pintelon, "Fast approximate identification of nonlinear systems", *Automatica*, 39, pp. 1267–1274, 2003.

T. Söderström and P. Stoica, *System Identification*, Upper Saddle River, NJ: Prentice Hall, 1989.

T. Van Gestel, J.A.K. Suykens, P. Van Dooren and B. De Moor, "Identification of stable models in subspace identification by using regularization", *IEEE Transactions on Automatic Control*, 46, pp. 1416–1420, 2001.

P. Van Overschee and B. De Moor, "N4SID: Subspace algorithms for the identification of combined deterministic-stochastic systems", *Automatica*, 30, pp. 75–93, 1994.

P. Van Overschee and B. De Moor, "A unifying theorem for three subspace system identification algorithms", *Automatica*, 31, pp. 1853–1864, 1995.

P. Van Overschee and B. De Moor, *Subspace Identification for Linear Systems: Theory, Implementation, Applications*, Norwell, MA: Kluwer, 1996.

M. Verhaegen, "Subspace model identification part 3. Analysis of the ordinary output-error state-space model identification algorithm", *International Journal of Control*, 58, pp. 555–586, 1993.

M. Verhaegen and P. Dewilde, "Subspace model identification part 1. The output-error state-space model identification class of algorithms", *International Journal of Control*, 56, pp. 1187–1210, 1992a.

M. Verhaegen and P. Dewilde, "Subspace model identification part 2. Analysis of the elementary output-error state-space model identification algorithm", *International Journal of Control*, 56, pp. 1211–1241, 1992b.

M. Verhaegen and D. Westwick, "Identifying MIMO Hammerstein systems in the context of subspace model identification methods", *International Journal of Control*, 63, pp. 331–349, 1996.

M. Verhaegen and X. Yu, "A class of subspace model identification algorithms to identify periodically and arbitrarily time-varying systems", *Automatica*, 31, pp. 201–216, 1995.

M. Viberg, "Subspace-based methods for the identification of linear time-invariant systems", *Automatica*, 31, pp. 1835–1851, 1995.

M. Viberg, B. Wahlberg and B. Otterstein, "Analysis of state space system identification methods based on instrumental variables and subspace fitting", *Automatica*, 33, pp. 1603–1616, 1997.

T.L. Vincent, P.P. Khargonekar, B.A. Rashap, F. Terry and M. Elta, "Nonlinear system identification and control of a reactive ion etcher", in *Proceedings of the American Control Conference*, Baltimore, MD, 1994, pp. 902–906.

J. Vörös, "Parameter identification of discontinuous hammerstein systems", *Automatica*, 33, pp. 1141–1146, 1997.

J. Vörös, "Parameter identification of Wiener systems with discontinuous nonlinearities", *Systems and Control Letters*, 44, pp. 363–372, 2001.

D.T. Westwick and R.E. Kearney, "A new algorithm for the identification of multiple input Wiener systems", *Biological Cybernetics*, 68, pp. 75–85, 1992.

D. Westwick and M. Verhaegen, "Identifying MIMO Wiener systems using subspace model identification methods", *Signal Processing*, 52, pp. 235–258, 1996.

T. Wigren, "Convergence analysis of recursive identification algorithms based on the Wiener model", *IEEE Transactions on Automatic Control*, 39, pp. 2191–2206, 1994.